

## Modeling structural mechanics of oyster reef self-organization including environmental constraints and community interactions

Simeon Yurek<sup>a,\*</sup>, Mitchell J. Eaton<sup>b</sup>, Romain Lavaud<sup>c</sup>, R. Wilson Laney<sup>d</sup>, Donald L. DeAngelis<sup>a</sup>, William E. Pine III<sup>e</sup>, Megan La Peyre<sup>f</sup>, Julien Martin<sup>a,g</sup>, Peter Frederick<sup>e</sup>, Hongqing Wang<sup>h</sup>, Michael R. Lowe<sup>i</sup>, Fred Johnson<sup>a</sup>, Edward V. Camp<sup>j</sup>, Rua Mordecai<sup>k</sup>

<sup>a</sup> U.S. Geological Survey, Wetland and Aquatic Research Center, 7920 NW 71 Street, Gainesville, FL, United States

<sup>b</sup> U.S. Geological Survey, Southeast Climate Adaptation Science Center, North Carolina State University, 127 David Clark Labs, Raleigh, NC, United States

<sup>c</sup> Institut des Sciences de la Mer, Université du Québec à Rimouski, 310 Allée des Ursulines, Rimouski, QC, G5L 2Z9, Canada

<sup>d</sup> U.S. Fish and Wildlife Service, Raleigh Ecological Services Field Office, Raleigh, NC, United States

<sup>e</sup> Department of Wildlife Ecology and Conservation, University of Florida, Gainesville, FL, United States

<sup>f</sup> U.S. Geological Survey, Louisiana Cooperative Fish and Wildlife Research Unit, School of Renewable Natural Resources, Louisiana State University, Baton Rouge, LA, United States

<sup>g</sup> U.S. Geological Survey, St. Petersburg Coastal and Marine Science Center, 600 Fourth Street S, St. Petersburg, FL, United States

<sup>h</sup> U.S. Geological Survey, Wetland and Aquatic Research Center, Baton Rouge, LA, United States

<sup>i</sup> U.S. Geological Survey, Great Lakes Science Center, Millersburg, MI, United States

<sup>j</sup> Fisheries and Aquatic Sciences Program, School of Forest Resources and Conservation, University of Florida, Gainesville, FL, United States

<sup>k</sup> U.S. Fish and Wildlife Service, Raleigh, NC, United States

### ARTICLE INFO

#### Keywords:

Self-organization  
Oyster reef  
Substrate  
Living shorelines  
Restoration  
Prediction

### ABSTRACT

Self-organization is a process of establishing and reinforcing local structures through feedbacks between internal population dynamics and external factors. In reef-building systems, substrate is collectively engineered by individuals that also occupy it and compete for space. Reefs are constrained spatially by the physical environment, and by mortality, which reduces production but exposes substrate for recruits. Reef self-organization therefore depends on efficient balancing of production and occupancy of substrate. To examine this, we develop a three-dimensional individual-based model (IBM) of oyster reef mechanics. Shell substrate is grown by individuals as valves, accumulates at the reef level, and degrades following mortality. Single restoration events and subsequent dynamics are simulated for a case study in South Carolina (USA). Variability in model processes is included on recruitment, spatial environmental constraints, and predation, over multiple independent runs and five predator community scenarios. The main goal for this study is to summarize trends in dynamics that are robust across this uncertainty, and from these generate new hypotheses and predictions for future studies. Simulation results demonstrate three phases following restoration: initial transient dynamics with considerable shell loss, followed by growth and saturation of the live population, and then saturation of settlement habitat several years later. Over half of simulations recoup initial shell losses as populations grow, while others continue in decline. The balance between population density, substrate supporting the reef, and exposed surfaces for settlement is mediated by overall population size and size structure, presence of predators, and relative amounts of live individuals and intact dead shells. The efficiency of settlement substrate production improves through time as population size structure becomes more complex, and the population of dead valves accumulates.

### 1. Introduction

Self-organization in natural systems is a process of establishing and maintaining a global pattern or structure through many cumulative interactions among individual agents of the system, which operate at a

local level without information regarding the broader global dynamic (Camazine et al., 2001). These agents follow a limited set of rules (Grimm and Railsback 2005), and are not governed by an overall plan or 'steering mechanism' (Young 2017). Instead, multiple positive and negative feedbacks reinforce their location and population dynamics.

\* Corresponding author at: U.S. Geological Survey, Wetland and Aquatic Research Center, 7920 NW 71 St., Gainesville, FL 32653, United States.  
E-mail address: [syurek@usgs.gov](mailto:syurek@usgs.gov) (S. Yurek).

These include proximal drivers, such as recruitment and interactions with substrate, and distal factors, such as environmental conditions, which impose external constraints on local resources (Klausmeier 1999). Organized aggregations form through collective activity of the agents, imposing negative feedback on adjacent areas by concentrating resources locally, and impeding resource flows externally. This leads to spatial patterning which ‘emerges’ from finer to larger scales (Levin 1992). Examples of self-organization include patterned geomorphology in mussel beds (Liu et al., 2014), arid land vegetation (Klausmeier 1999), wetland vegetation (Watts et al., 2010), and savannahs (Jeltsch et al., 1998), signaling networks in termites and slime molds (Bignell et al. 2010; Camazine et al., 2001), murmuration in birds (Reynolds 1987), and shoaling in fish (Huth and Wissel 1992). In the example of mussel beds, dispersal and aggregation of mussels are the main drivers determining bed geomorphology, but exogenous factors of sediment and wave energy also influence the pattern set by the mussels, as the beds concentrate sediment and absorb wave inputs, leading to regularly spaced, linear beds.

In this study, we focus on self-organization of the reef-building system of the Eastern oyster (*Crassostrea virginica*), which is native to the Atlantic and Gulf of Mexico coasts of the United States. Our main goal is to examine mechanical properties of the evolved reef system that are shared across locales. Although oysters are traditionally valued as an important economic commodity, reef ecosystems are gaining increasing attention for their resilience and self-maintenance properties, which provide significant ecological and conservation value. Reefs function as foundation habitats supporting aquatic food webs, and potentially provide numerous other ecosystem services, such as nutrient regulation, storage, and wave attenuation (Coen et al., 2007; Grabowski et al., 2012). These services likely benefit adjacent habitats, such as salt marsh, by mitigating erosion and stabilizing shorelines (Arkema et al., 2013; Piazza et al., 2005; Scyphers et al., 2011). For these reasons, restoration of reefs for ecosystem-based management is growing in practice (Currin et al., 2010; Frederick et al., 2016). The success of these restorations hinges on the ability to understand and predict the mechanisms that lead to self-organizing and self-sustaining reefs.

The key proximal drivers for generating oyster reef structure are production of calcareous shell substrate by oysters, and recruitment of oyster larvae to the reef. The key external factors are wave energy, food, predation, sedimentation, and environmental conditions, such as water temperature and salinity, which influence individual metabolism, growth, reproductive output, and survival. Shell is grown by individuals as articulating valves, and accumulates at the population level following individual mortality, where it begins to break down. Settlement patterns of larvae represent positive feedbacks that reinforce the reef structural pattern (Bartol and Mann 1997). Larvae are attracted to the reef by chemical and auditory cues (Lillis et al., 2015), settling on previously deposited substrate or other live oysters, and forming clusters which grow in volume both vertically and horizontally. Feedbacks between external factors and internal processes are possible. For example, as the oyster population and reef increase in size, the combined surface area of shell serving as settlement habitat increases, representing positive feedback, however, the community of predators attracted to the reef also increases, imposing negative feedback, but at the same time exposes shell surfaces for new recruits. Larger adult oysters impede settlement to some extent by occupying a portion of reef substrate, but also themselves serve as substrate for recruits. Thus, the balance between individual competition for space on the reef and collective generation of new space at the population level is complex, particularly given the spatial and environmental limits on reef growth. Similar interactions with hydrology are possible. Water becomes channeled as it flows over and around the reef, which increases the flux of food particles (Lenihan 1999), but negatively impacts settlement conditions such as through increased turbulence (Bahr and Lanier 1981). These feedbacks act on different components of the reef (i.e., adults, larvae, shell), and when maintained in balance, ensure that sufficient materials and energy are exchanged

among components.

The primary ecological question for oyster reef self-organization concerns how proximal drivers and external factors combine to maintain a net balance of reef shell (positive, negative, or zero), and whether this coincides with growth or decline of the live population (Powell and Klinck 2007). Shell degrades through natural physical erosion and chemical dissolution (Powell et al., 2006), which must be offset by production of shell by live individuals. Mortality of live individuals negatively impacts shell production but positively supports both larval settlement, by opening up interstitial surfaces, and substrate accumulation, as shell breaks down and consolidates. This successional dynamic of shell and reef structure, driven by oyster mortality, can be considered a chain of multiple interacting feedbacks. Another important condition is that oyster reefs occur in highly dynamic, spatially constrained environments, thus the volumes attained by both the crushed shell foundation layer, (i.e., degraded oyster valves) and productive outer live layer are limited. The shell foundation is limited by external factors such as water depth and shoreline geomorphology, while the live population is limited by the ability of oysters to aggregate and form clusters. When either of these limits are reached and growth of the reef ceases, mortality may play a key role in renewing the chain of feedbacks by opening up space for new recruits. The question then is what balance of these dynamic mechanisms is required to sustain the live population, while also maintaining shell accumulation on the reef?

We examine this question by developing an individual-based model (IBM) of oyster reef-building dynamics that specifically considers reef three-dimensional structure. Our overall goal is to gain insights into how the live oyster population, reef structure, and larval recruits interact through time as a coupled system, to converge on stable dynamics that sustain the reef. We specifically focus on the successional process of shell habitat generation, from live production and growth, to accumulation of valve and crushed shell from dead oysters. We consider two, somewhat distinct roles of habitat: one supporting the live population, elevating it above the sea floor, and the other supporting reproduction through exposed settlement substrate. Since the mechanics of these are quite different – consolidating biomass at the reef scale versus exposing individual shell surfaces – we explicitly represent each process in the model at its respective scale. We then develop hypotheses and predictions on how the live population might interact with habitat through time at these two scales, particularly under environmental spatial constraints. We first assume that reef self-organization generally hinges on the efficiency of the reef to generate both types of shell habitat, cycling shell through its roles as settlement area and then reef substrate. We then assume that demographic structure is also important, since larger individuals produce more larvae and larger, longer-lasting shell. However, in both cases, we make no assumptions on what dynamics or patterns emerge at the population and reef level. To our knowledge, this is the first attempt to model the three-dimensional structure of oyster reefs as a function of individual dynamics, similar to previous studies on corals (Sleeman et al., 2005) and macroalgae (Yniguez et al. 2008).

We apply the oyster reef IBM to simulate reef restoration at a study location in North Inlet, Winyah Bay, SC (USA), using a time series of environmental conditions which vary seasonally and interannually. We first validate model results against an empirical growth study conducted at this site (Dame et al., 2000), and then develop a biological ensemble modeling approach (Gårdmark et al., 2013) to evaluate restoration performance, where single restoration events and their ensuing dynamics are simulated over multiple runs, with variation included on select model assumptions and processes. Variability in larval settlement rate, predation, and a constraint on live population volume are applied within ranges that sustain populations and do not force extinction, which is beyond the scope of this study. Predation is represented in five scenarios, where community membership and the sizes of oyster prey targeted by each predator group are varied, including a scenario with no predators. Model dynamics are then summarized across simulations as population level measures of individual density, total biomass, and

habitat settlement area through time, providing a quantitative evaluation of restoration performance with associated ranges of uncertainty. Finally, the role of population demography in stock-recruitment dynamics is examined by comparing availability of settlement habitat to population-level measures of live biomass and density of larger individuals, across simulations.

## 2. Methods

The oyster reef individual-based model is described following the ODD protocol (*Overview, Design concepts, and Details*; Grimm et al., 2006, 2010, Railsback and Grimm 2019). This format begins with a plain language description of model processes, interactions, and scales, followed by additional details. The full ODD is given in *Supplement 1*. Here we present a summary version, with some wording repeated following ODD recommendations.

### 2.1. Overview

To simulate oyster reef-building dynamics, we develop an integrated model that separately tracks the life cycles of individual oysters (somatic tissue, gonad, and shell), the half-lives of shell valves following mortality, and the accumulation of crushed shell matter. All together, these combine to form a three-dimensional reef. In this way, dynamics of the model self-organize across levels of the individual, population, and reef structure. The model also demonstrates the importance of predation in sustaining recruitment and habitat availability, and thus stable development of the reef system.

There are two sets of *entities* (i.e., autonomous objects or actors): individual live oysters and shell valves (Fig. 1). Live oysters grow shells which remain as substrate when the oyster dies (here ‘valve’ indicates only the dead state). The dynamics of these two entities are described by *state variables* of volume (cm<sup>3</sup>), energy (J), age (years), and vertical location on the reef (cm). Following mortality, physical state variables carry over from live oyster to valve, and the valve then begins to degrade through erosion and dissolution, eventually reaching a size where concavity is assumed to be lost and it is no longer considered an individual (< 5 cm, chosen arbitrarily). These shell remnants constitute another single state variable of crushed oyster shell material, tracked as a total biomass pool. External factors impacting individuals are salinity, temperature, food availability, predators, and burial. Population and reef level variables are *observed* as aggregates of individual state variables. The *spatial extent* is the reef itself (tens of m<sup>2</sup>), which is a dynamic entity with rectangular, three-dimensional morphology and sloping vertical sides (Fig. 2). Crushed shell comprises the bulk of the physical volume of the reef, while the live oysters and valves lie on the outer surface (top

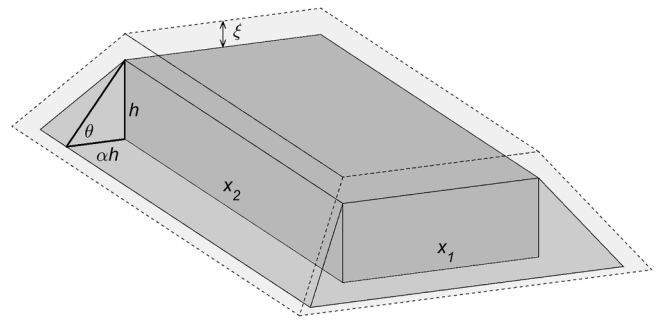


Fig. 2. Reef geomorphology generalized as a trapezoidal volume. Dark gray volumes represent the space occupied by crushed shell. Light gray and dotted lines represent the volume occupied by live oysters and valves. Crushed shell is assumed to accumulate within the rectangular base volume with fixed horizontal dimensions,  $x_1$  and  $x_2$ , spilling over to form the adjacent triangular volume.

and sides, see Fig. 2). *Temporal extent* of simulations is 22 years, and *temporal resolution* is in daily time steps. Discrete difference equations model dynamics at this time scale, approximating dynamics at the weekly to monthly scale, which is generally the resolution at which these resources are monitored (Table 1).

### 2.2. Design concepts and selected details

The main *processes* in the model are the life cycle dynamics of the live population (growth of tissue and shell, reproduction, and mortality), and substrate dynamics (accumulation and degradation), which together determine the *emergent property* of reef morphology and structure. Live individuals grow according to rules of energy acquisition and allocation defined by Dynamic Energy Budget theory (Kooijman 2010; Lavaud et al., 2017). Energy is first assimilated into reserve and then partitioned between somatic growth and reproduction (Equations 1–8, A1–14, Supplement 2). These dynamics are modeled on discrete time steps of one day, approximating continuous growth at the scale of weeks. Over time, individuals transition through phases of birth, metamorphosis, and puberty, defined by maturity thresholds, and experience a metabolic acceleration between birth and metamorphosis (‘abj’ model in DEB terms). Maintenance energetic costs of somatic tissues and maturity must be met before the remaining energy can fuel structural growth or gamete production. All energy fluxes are mediated by temperature, which generally increases metabolism, and food intake is additionally mediated by salinity, where feeding rates decline to zero from 10 to 3 psu (Lavaud et al., 2017). Physiological variability among

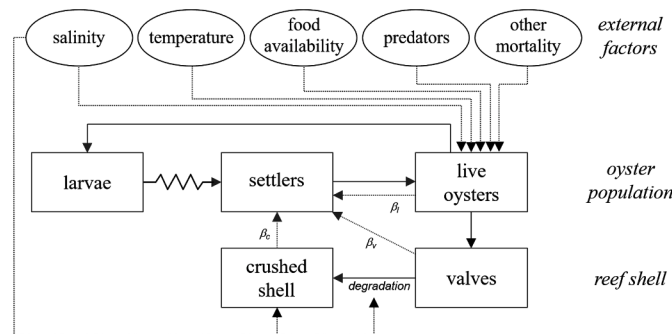


Fig. 1. Conceptual representation of the oyster reef individual-based model (IBM). Boxes represent components of the oyster population and the shell biomass of the reef. Solid arrows indicate transfers between these groups. Ovals and dotted lines represent external factors influencing oyster dynamics. Settlement from the larval population onto the reef is limited by a filter (zig zag arrow) on settlement density (settlers m<sup>-2</sup>), which is a function of the surface area of crushed reef shell, intact shell valves, and living oysters, parameterized by  $\beta$ . All dotted line relationships are described by parameterized mathematical functions (see text).

**Table 1**  
Dynamic equations of oyster reef IBM.

Dynamic Energy Budget	
$\frac{dV_i}{dt} = \frac{\dot{p}_G}{E_G} - \dot{p}_{LV}$	Individual structural volume (see Table 2) (1)
$\frac{dE_i}{dt} = \dot{p}_A - \dot{p}_C$	Individual energy reserves (2)
$\frac{dE_{Ri}}{dt} = \dot{p}_{R\kappa R} - \dot{p}_{LR} - E_{sp}$	Individual reproduction buffer (3)
$\frac{dE_{Hi}}{dt} = \dot{p}_H$	Individual maturity (4)
$L_{wi} = \frac{V_i^{1/3}}{\delta_M}$	Individual shell length (5)
$W_{di} = V_i + (E_i + E_{Ri}) \frac{W_E}{\mu_E}$	Individual tissue wet weight (6)
$W_{Si} = \eta_S \left[ V_i + \frac{\phi_{valve}}{\phi_{tissue}} (E_i + E_{Ri}) \frac{W_E}{\mu_E} \right]$	Individual valve wet weight (proportional to tissue) (7)
$\phi_{valve.tissue} = c \frac{1}{b^a \Gamma(a)} T_i^{a-1} e^{-T_i/b}$	Theoretical scaling function (Rodhouse 1978) $T_i$ is individual age in years, $\Gamma$ is gamma function (8)
Population and reef dynamics	
$O_{t+1} = \{O_t \mid m_{ij} = 1, p_{ik} = 1\} \cup settlers_t$	Population of live oyster individuals (9)
$S_{t+1} = \{S_t \mid W_{Sit} - r_{deg} W_{Sit} > \psi\} \cup Snew_t$	Population of valve individuals (dead shell) (10)
$\frac{dW_C}{dt} = \sum_{i \in C} \delta_{Ci} W_{Sit} - r_{deg} a_C W_{Ct}$	Crushed reef shell ( $a_C$ = proportion exposed, see S3.5) (11)
$r_{deg.v} = rmin + \sigma_{sal} a \frac{rmax - rmin}{rmax^b}$	Shell degradation rate, $\sigma_{sal}$ = salinity variance (3 days) (12)
$V_{Ct} = \frac{W_{Ct}}{\eta_c}$	Crushed shell volume including void space (13)
$x_1 x_2 h + x_1 a h^2 + x_2 a h^2 + \frac{4}{3} \alpha^2 h^3 - V_{Ct} = 0$	Function solving for reef height, $h$ , from volume (14)
Reproduction and Settlement	
$\frac{dLarv}{dt} = r_{larv} Larv - settlers_t + \sum_1^{n_{rem}} \frac{E_{sp}}{\mu_{egg}}$	Larval population (15)
$R_t = \max(\rho H_t, Larv)$	Total settlers per time step (larvae to reef) (16)
$H_t = H_c + H_v + H_l \mid Vocc_l + Vocc_v < \xi$	Total available settlement habitat (17)
$H_c = \beta_c (A_c - Aocc_{vc} - Aocc_{lc})$	Available settlement habitat on crushed shell (18)
$H_v = \beta_v (\sum_1^n A_{vi} - Aocc_{lv})$	Available settlement habitat on valve (19)
$H_l = \beta_l (\sum_1^n A_{li} - Aocc_{ll})$	Available settlement habitat on live oysters (20)
$A_c = x_1 x_2 + 2\sqrt{h^2 + (ah)^2} (2ah + x_1 + x_2)$	Total reef surface area (crushed shell) (21)
$A_{vi} = 2\delta_{width} L_{wi}^2$	Individual live oyster surface area (22)
$A_{li} = 4\delta_{width} L_{wi}^2$	Individual valve surface area (23)
$Aocc_{li} = \sum_1^n \pi (\delta_R L_{wi})^2$	Total area occupied by live oysters (on all three types) (24)
$Aocc_{vc} = \sum_1^{n_v} \delta_{width} \delta_{depth} L_{wi}^2$	Total area occupied by valves (on crushed shell, $c$ ) (25)
$Vocc_l = \sum_1^n \pi (\sigma_i \delta_R L_{wi})^2 L_{wi}$	Total volume occupied by live oyster population, $O_t$ (26)
$Vocc_v = \sum_1^{n_v} \pi \left(\frac{\delta_{width}}{2} L_{wi}\right)^2 L_{wi}$	Total volume occupied by valve population, $Q_t$ (27)
Predation and mortality	
$P_{nm} = a e^{-be^{-c(V_i-d)}}$	Probability of natural mortality (28)
$t_{term} = 365(c + a(-\ln(1 - PR_t))^{1/b})$	Terminal age (29)
$P_b = 1 - e^{-ae^{-b(\delta_h - c)}}$	Probability of burial ( $\delta_h$ = elevation difference) (30)
$Vul_{i,k} = c \frac{1}{b^a \Gamma(a)} V_i^{a-1} e^{-V_i/b}$	Vulnerability of oyster prey to each predator type, $k$ (31)
$Pred_k = pred_{max} e^{-a_{pk} Prey_{max}/Prey_{vul,k}}$	Predator density ( $m^2$ , $Prey_{vul}$ = vulnerable prey density) (32)
$f_{pred,k} = \frac{cons_{prey,k} Prey_{vul,k}}{(1 + cons_{prey,k} h_k Prey_{vul,k} + w_k Pred_k)}$	Functional response of predator $k$ on oyster (33)
$P_{f,k} = \frac{1}{(1 + (a-1)e^{-bh})}$	Temperature-dependent foraging scalar (34)
$P_{occ,k} = a \frac{1}{(1 + (b-1)e^{-c})(1 + (b-1)e^{-c})} > PR_k$	Temperature and salinity-dependent predator occurrence logical (PR = pseudorandom draw) (35)
$ncons_k = P_{occ,k} P_{f,k} Pred_k f_{pred,k} x_1 x_2 dt$	Total oyster prey consumed by each predator group, $k$ (36)

individuals is introduced by applying *stochastic* variation to selected metabolic parameters:  $\{p_{Am}\}$ ,  $\{p_M\}$ , and  $X_K$  (Tables 2 and S1). The survival or mortality of all individual live oysters at each time step is described by a set of equations relating probability of survival to individual size or elevation on the reef (Equations 9–10, 28–34, also described later).

Reproduction is modeled as linked *processes* of spawning, maintenance of a pelagic larval population, and settlement from this population to the reef (Equations 15–27). These are tracked respectively as *aggregated variables* of eggs released, larvae, and settlers per time, without individual attributes. Together they simulate pelagic dynamics of the oyster population at the time scale of ~20 days (Deksheniaks et al.,

2000). The larval population is maintained as the net balance of input from spawning and export through settlement, with a fixed population level decay rate. In this study, it functions as a closed auto-recruiting system. Spawning is generally a short-term event (days to weeks), and events can recur as long as temperature and gamete production are sufficient. Spawning is initiated when thresholds of temperature and population-level gonado-somatic index (GSI) are exceeded. Gametes are released by individuals through the DEB *submodel*, and total eggs are summed and input to the larval population. Settlement represents a transient phase during which recruits enter the live population and become specified as individual oysters. Settlement involves two *collectives*, or subsets of agents with unique actions: settlers, a subset of the

**Table 2**  
DEB flux equations.

$\dot{p}_A = \{\dot{p}_{Am}\}fV_i^{2/3}c_Sc_T$	Assimilation rate	(A1)
$\dot{p}_C = E_C \frac{E_G \dot{v}_C V_i^{2/3} + \{\dot{p}_M\}C_T}{\kappa E_i + E_G V_i}$	Mobilization rate	(A2)
$\dot{p}_M = \{\dot{p}_M\}c_T V_i$	Somatic maintenance rate	(A3)
$\dot{p}_J = E_{Hh} k_J c_T$	Maturity maintenance rate	(A4)
$\dot{p}_H = \max(0, (1 - \kappa)\dot{p}_C - \dot{p}_J)$ if $E_{Hh} < E_H^p$ , otherwise 0	Allocation to maturation	(A5)
$\dot{p}_R = \max(0, (1 - \kappa)\dot{p}_C - \dot{p}_J)$ if $E_{Hh} \geq E_H^p$ , otherwise 0	Allocation to reproduction	(A6)
$E_{sp} = E_{Ri} \kappa_{sp} \max_{gam}$	Spawned energy (via eggs)	(A7)
$Sk = \max(0, \dot{p}_M - \kappa \dot{p}_C) + \max(0, \dot{p}_J - (1 - \kappa)\dot{p}_C)$	Deficit in maintenance energy (shrink)	(A8)
$\dot{p}_{LR} = \min\left(Sk, \frac{E_{Ri} \kappa_R}{dt}\right)$	Lysis of reproduction buffer	(A9)
$\dot{p}_{LV} = \min\left(Sk - \dot{p}_{LR}, \frac{dV V \mu_V}{w_V dt}\right)$	Lysis of structure	(A10)
$\dot{p}_G = \max(0, \kappa \dot{p}_C - \dot{p}_M)$	Allocation to growth	(A11)
$c_T = \exp\left(\frac{T_A}{T_{ref}} - \frac{T_A}{T}\right) \frac{1 + \exp\left(\frac{T_{AL}}{T_{ref}} - \frac{T_{AL}}{T}\right) + \exp\left(\frac{T_{AH}}{T_H} - \frac{T_{AH}}{T_{ref}}\right)}{1 + \exp\left(\frac{T_{AL}}{T} - \frac{T_{AL}}{T_L}\right) + \exp\left(\frac{T_{AH}}{T} - \frac{T_{AH}}{T_{ref}}\right)}$	Temperature correction based on the Arrhenius relationship	(A12)
$c_S = \frac{S - S_L}{S_H - S_L}$ if $S_L > S > S_H$ 1 if $S > S_H$ 0 if $S < S_L$	Salinity correction factor for feeding only	(A13)
$f_{chla} = \frac{chla}{chla + X_K}$	Functional response of oyster on chlorophyll $\alpha$	(A14)

live population, and available settlement habitat, a subset of shell types (live, valve, and crushed). Input of settlers from the larval to the live population is described by the settlement rate,  $\rho$ , multiplied by the summed area of exposed shell surfaces not occupied by other entities. In this way, the settler *collective* is conditioned by the settlement habitat *collective*. Natural variability in settlement (i.e., larvae locating and navigating to the reef) is represented by varying rate,  $\rho$ , in simulations for each spawning event and at the daily scale (see Section 2.4 and Supplement S1.15). Settlement continues until larvae or settlement substrate are expended, generally days to weeks following spawning.

The net balance of crushed shell is determined by two processes of gain of new crushed shell material through degradation of valves, and losses through degradation of existing crushed shell (Equations 11–12). The gradual degradation of valves into crushed shell is described by a rate linked to salinity variance, which is a proxy for exposure to estuarine processes (e.g., redox reactions, dissolution, erosion; Day et al., 2012, Powell and Klinck 2007). Loss of crushed shell is described similarly, although only shell along the outer surface of the reef not covered by other oysters or valves is considered exposed to degradation (see Supplement 1). In this way, the total shell budget is tracked through time, concurrently for all three shell types (Equations 9–11).

Reef geomorphology is a generalized trapezoidal volume comprised of crushed shell (Fig. 2, solid lines), with live oysters and valves occupying the upper surface (dotted lines). Reef dimensions are derived by converting crushed shell weight to volume and solving for height,

assuming fixed base dimensions,  $x_1$ ,  $x_2$ , and a triangular overflow volume with angle of repose,  $\theta$ , and width proportional to height (Equations 13–14). The volume of the ‘live layer’ occupied by oysters and valves is limited by an assumed hydrodynamic *constraint*, described by vertical parameter,  $\xi$ , multiplied by the surface area of the reef trapezoid (Equations 21, 26–27). Settlement ceases whenever this volumetric limit is reached. The individual volume of each live oyster and valve is described by a cylinder. Live oysters are assumed to have a ‘zone of influence’ extending beyond their physical dimensions which implicitly represents natural spacing maintained among oyster individuals. When taken collectively at the population level, this also represents spacing among oyster clusters. The live layer is therefore not entirely filled with oyster and shell biomass, but has some empty space. Valves have a radius equal to only their physical width.

The demographic size structure of the live population is *observed* by taking daily measures of individual density (number  $m^{-2}$ ), binned within four size classes used by Wang et al. (2008): *spat* (< 25 mm), *juvenile* (25–50 mm), *adult* (50–75 mm), and *sack* (> 75 mm). The *sack* class represents market size oysters, although no harvest is assumed here. Note these designations are for observation only and are not used in model processes. Variables describing dynamics at the reef level are total shell biomass (kg), reef height (cm), volume ( $m^3$ ), and exposed surface area for settlement ( $m^2$ ). Reef performance and uncertainty across simulations are observed as daily means and quantiles ( $\tau = 0.1, 0.5, 0.75, 0.9, 0.98$ ) of these variables, taken at each time step.

**Table 3**  
Characterization of predator foraging behavior types.

	Predator 1	Predator 2	Predator 3	Predator 4
Foraging type	Small polyhaline invertebrate or fish	Intermediate pan-estuarine resident invertebrate, demersal fish	Large transient pan-estuarine invertebrate, demersal fish, avian	Marine fouling
Target prey	Spat	Juvenile	Juvenile, adult	Juvenile, adult
General occurrence	High (0.7)	Low (0.2)	Low (0.22)	High (0.8)
Temperature occurrence	> 10 °C	> 10 °C	> 10 °C	> 20 °C
Salinity occurrence	Poly-euhaline	Meso-poly-euhaline	Meso-poly-euhaline	Euhaline
Predator density response	High	Intermediate	Low	Low
Consumption rate (oysters $m^{-2}$ )	Low (0.8)	Low (0.1)	Intermediate (2)	High (8)
Handling time (d)	Low (0.25)	High (2)	Low (0.25)	Intermediate (1)
Self-interference	Low (2)	Low (1)	High (10)	None (0)

Predation in this study represents an external driver that facilitates turnover of shell from live to dead valves, exposing shell surfaces for settlement and initiating shell degradation. Predation is thus a *Design concept* that affects mechanics at the reef scale, and individual *fitness* through survival. Importantly, predation is intended as the collective action of a community of predators, and not any single species. Predators are therefore represented as characterizations of foraging behavior types (i.e., guilds with similar foraging traits), which have different levels of activity related to environmental conditions and which target different-sized oyster prey (Holling 1959), thereby exposing varying sizes of valves on the reef (Equations 31–36). In this way, the predator community responds dynamically to changes in oyster population abundance and size structure, as well as to changes in environmental conditions. Table 3 describes four foraging types applied in this study, derived from field and laboratory studies (Brown and Richardson 1988; Brown et al., 2008; Butler 1985; Eggleston 1990; Grabowski et al., 2008; Haller-Bull et al. 2019; Hesterberg et al., 2017; Kennedy et al., 2009, Newell et al., 2007, O'Connor et al., 2008, Speights and McCoy 2017, Stephenson et al., 2013, Stempien 2007).

Total prey consumed by each predator group is determined by predator occurrence, density, and functional response taken together. Predator occurrence is related to temperature and salinity through sigmoid equations (Lord 2014, Menzel and Nichy 1958). Predator densities are related to their oyster prey density by saturating functions. Per predator extraction of prey is described by functional response equations (Beddington 1975, DeAngelis et al., 1975, Holling 1959). Parameter values for occurrence and functional response are selected so that feeding activity of the groups are somewhat uncorrelated. These are based on specific studies when available, and descriptive life history otherwise (see Supplement S1.10). Our goal is to represent reasonable ranges of predation that impact dynamics of the system but do not drive the population to extinction. Natural variability in predator use of the reef is represented in simulations by varying parameter,  $pred_{max}$ , which determines the magnitude of densities (Equation 32). This is implemented concurrently with variation in settlement parameter,  $\rho$ , but independently, producing partially decoupled dynamics in the predator-prey function (see Section 2.4, Supplement S1.15, and Figure S1.1). In addition to predation, other mortality factors include natural mortality (i.e., survival to adulthood), probability of burial (implicitly representing sedimentation), and terminal age (Equations

28–30), in which survival is related to individual size or elevation on the reef (Harding et al., 2008, Lorenzen 2000, Nestlerode et al., 2007, Camp et al. 2015, Powell et al., 1994).

### 2.3. Initialization

In this study, the model is *initialized* to simulate restoration actions for an example location in North Inlet, Winyah Bay, SC (USA), a coastal estuarine and salt marsh ecosystem with regular tides and low fresh-water input (Dame et al., 2000). Single restoration events are simulated at the beginning of runs, and restoration performance is tracked over subsequent decades (1996–2018). No further management actions are taken following the initial restoration. Reefs are stocked on the initial time step of runs with crushed shell equivalent to a height of 40 cm ( $5.158 \times 10^3$  kg). Individuals are stocked at a density of 400 individuals  $m^{-2}$  with initial individual DEB volume at birth,  $V_b$ , of  $8 \times 10^{-9}$   $cm^3$ . Reef base dimensions,  $x1$ ,  $x2$  (Fig. 2), are fixed at  $10 \times 2$  m.

Inputs for simulations are time series of salinity (psu), temperature ( $^{\circ}C$ ), and chlorophyll  $a$  ( $\mu g L^{-1}$ ), representing physical environmental conditions and food source. These were recorded at Oyster Landing (OL, 33.349 $^{\circ}N$ , 79.189 $^{\circ}W$ ) in North Inlet, SC, from January 1, 1996 to August 1, 2018 (Fig. 3 and Supplement 1). Due to limited availability of chlorophyll data, a derived single-year time series is applied equally across years. These data sets are managed by the University of South Carolina's Baruch Institute for Marine and Coastal Science, as part of the NOAA National Estuarine Research Reserve System (NEER, <http://cdmo.baruch.sc.edu/dges/>).

### 2.4. Ensemble modeling and parameter variation in simulation runs

The oyster reef IBM is implemented in an ensemble modeling framework, in which underlying processes that determine reef dynamics are varied over multiple simulation runs, with a goal of identifying long-term trends in the reef that are robust over model uncertainty and natural variability in these processes. Here, variation is applied on predation, larval settlement, and the hydrodynamic constraint on the reef live layer. Functions describing these processes are varied by drawing key parameters from probability distributions, which generally adjusts the magnitude of the function but not its form (see Supplement S1.15). This approach characterizes both natural variability of the ecosystem,

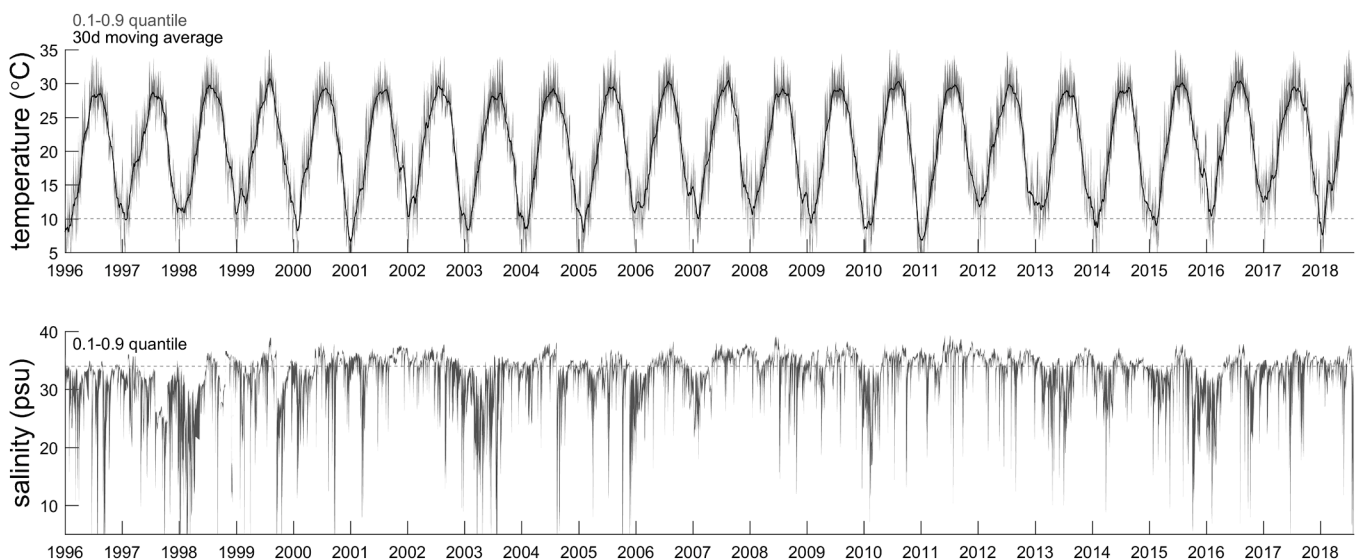


**Fig. 3.** Time series of temperature ( $^{\circ}C$ ) and salinity (psu) recorded at Oyster Landing, North Inlet, Winyah Bay, SC (NIWOL), between 1996 and 2018. Top panel: (light gray band) daily quantile distribution of temperature for range  $\tau = 0.1$ – $0.9$ , and (black line) moving average of daily temperature with a 30-day sliding window. Bottom panel: daily quantile distribution of salinity for same range of  $\tau = 0.1$ – $0.9$ . Dotted line in top panel indicates an important threshold where predator occurrence and functional response reduce considerably. Dotted line in bottom panel represents an approximate threshold for marine conditions (34 psu).

through the behavior of the distributions, and parametric uncertainty of model functions, by drawing select parameter values from distributions. The hydrodynamic constraint is varied by drawing parameter,  $\xi$ , which regulates live layer depth (Equation 17), from a uniform distribution, truncated between 10 and 30 (cm). Note that this constraint is implemented as a volume-based threshold. Values below 10 cm generally lead to reef decline in the model. Settlement patterns are varied across runs by adjusting the overall magnitude of rate parameter,  $\rho$  (Equation 16), in addition to variation within runs as described earlier. Predator densities are varied similarly to settlement, but only within runs. Finally, effects of predator community composition are examined by developing five scenarios with varying predator membership: all Predators, no Predators, Predators 2 and 3 only, Predators 1–3, and Predators 2–4. A total of 1,200 separate simulation runs are conducted for each scenario.

## 2.5. Model validation and sensitivity analysis

The individual-based modeling approach is designed to avoid biases of population-level assumptions by simulating individual-level mechanistic processes in detail, whenever possible. However, assumptions at this level are necessary. We examine these with two separate sets of simulations, a model validation and sensitivity analysis. Individual growth in our DEB *submodel* is validated against actual growth measurements collected during a comprehensive two-year field study of tidal creek ecology (CREEK, Dame et al., 2000), which commenced the NEER research program in North Inlet. In this study, eight sites in Clambank and Town Creeks (adjacent to OL) were sampled, and growth was measured as change in shell length (mm) over regular  $\sim 30$  day intervals

(data portal, <https://www.baruch.sc.edu/biological-databases>). Our simulations follow the same deployment and retrieval schedule of the CREEK study (see Supplement 3), using physical data from the nearby NEER Clambank Creek station (CC, 33.334°N, -79.193°W).

The sensitivity of simulated oyster reef dynamics to key modeled underlying processes is also examined. These include predation, settlement, and the hydrodynamic constraint, which are varied in the ensemble framework, and additionally, the assumption that the surface area available for settlement on valves is greater than on live oysters. This analysis is structured following the same methods as the ensemble modeling, implementing multiple simulations with variability across and within runs, however, in the sensitivity analysis, each function is additionally varied, independently. For the first three processes, the parameters governing the probability distributions (e.g., shape and scale parameters) from which key function parameters are drawn, are alternately increased and decreased, thereby shifting the range of the function parameters without changing functional form. This preserves the modeled variability in these underlying processes, while testing sensitivity of the model to the assumptions of the distributions (see Supplement S1.15 for details). Parameters of the gamma and Rayleigh distributions are adjusted by  $\pm 20\%$ , and the range of the uniform distribution is shifted by  $\pm 25\%$ . Sensitivity to valve settlement area is examined by using the same constant of 2 in both Equations 22 and 23, replacing 4 in the equation for valves. Only the scenario with all predators is considered for these sensitivity analyses, totaling seven separate ensembles (i.e., three processes varied in two directions). Modeled oyster reef dynamics of the sensitivity analyses are then compared to the original results.

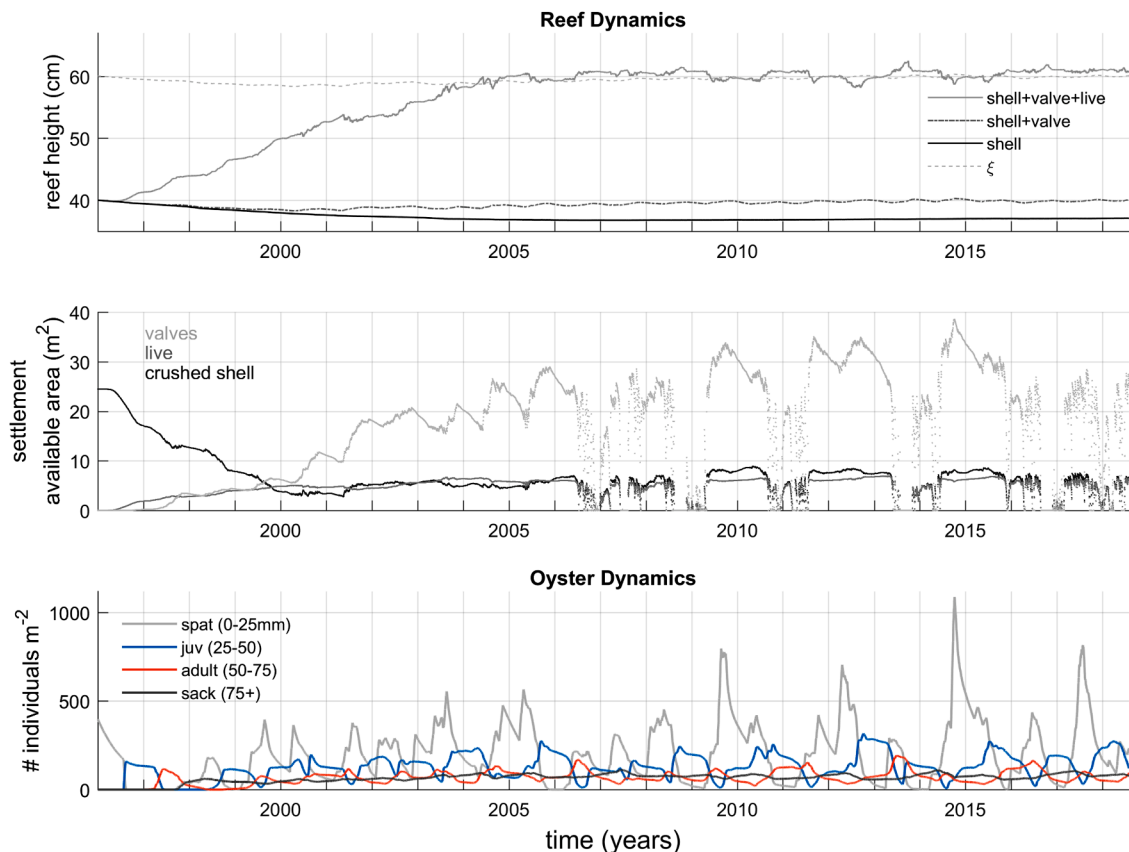


**Fig. 4.** Example of model outputs from a single simulation run. Top panel shows the reef height in cm, measured for: crushed shell only (black line), crushed and valves (dark gray dotted line), and crushed, valves, and live oysters (light gray line). Note void volume for live oysters is higher than other shell types. Light gray dotted line represents the approximate analogous height,  $\xi$ , through time, of the volumetric threshold constraint on the live oyster population. Middle panel shows shell surface area available for settlement for three shell types: live oysters (dark gray), valves (light gray), and crushed shell (black). Bottom panel shows the size structure of the oyster population through time. (For interpretation of the references to color in this figure legend, the reader is referred to the web version of this article.)

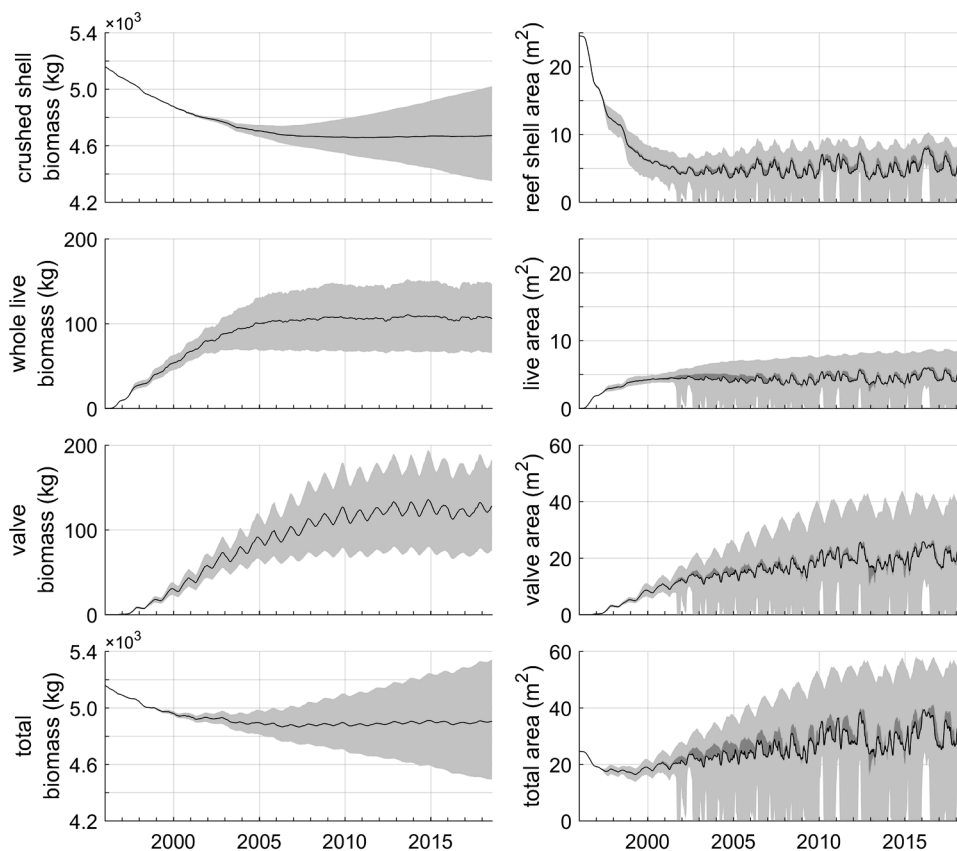


**Fig. 5.** Oyster reef biomass (kg) and settlement habitat ( $\text{m}^2$ ) through time (1996–2018) for scenarios with predators. These variables are shown separately for each shell type (crushed, live, and valve; top three rows), and for all types combined (bottom row). Live biomass includes somatic tissue, gonad, and shell. All variables are summarized as daily quantile distributions over  $\sim 1,200$  runs for each scenario (light gray bands,  $\tau = 0.1 - 0.9$ ). Black lines indicate daily means, and dark gray bands indicate difference between mean and median (right column only), which shows whether most of the data points lie above or below the mean.

### 3. Results

#### 3.1. Environmental conditions

The temperature time series used in simulations (Fig. 3) has considerable interannual variability, with several abrupt changes between adjacent years, most notably in winter (e.g., 2002, 2012, 2017). Interestingly, the coldest winter in 2011 is preceded by one of the hottest summers in 2010. The overall salinity regime for this estuary is generally euhaline (30–40 psu), with intermittent polyhaline (18–30 psu), and infrequent mesohaline periods (5–18 psu). Note that the experimental salinity levels used to calibrate the DEB model parameters in Louisiana focus on the mesohaline range (3–25 psu, Lavaud et al., 2017), which is not prevalent in North Inlet, SC. Thus, the salinity correction on DEB processes in simulations has minimal effect here.

#### 3.2. Oyster reef dynamics (single example)

An example of simulated dynamics for a single oyster reef are shown in Fig. 4. Crushed shell settlement area (dark line, middle panel) is highest at the beginning of runs when it is largely unoccupied (1996), gradually declines as the live oyster population grows and covers it, and stabilizes around 2000. In the following years (2000–2013), settlement area on live oysters and valves increases as these populations increase. Total settlement habitat on valves fluctuates annually, attaining approximately 3 to 6 times that of live oysters toward the end of runs (2010 to 2018). Note that calculations of individual surface area differ only by a factor of two (Equations 22–23). Settlement area on valves and live oysters stabilizes between 2010 and 2015. Beginning in 2006, all values of settlement area fall to zero when the total volume determined by parameter,  $\xi$ , multiplied by reef surface area is exceeded (dotted line, top panel). To visualize this threshold,  $\xi$  is shown here as an approximate height derived from this dynamic volume, however, it is not

entirely analogous to other heights shown. Cohort dynamics of the live population (bottom row) are observed as changes in densities within size classes (number  $\text{m}^{-2}$ ). In this example, larger individuals (adult, sack) remain relatively stable across years as they are replenished by recruits, although recruitment varies considerably across years and within seasons. For example, see large peaks of spat in 2009, 2014, and 2015.

#### 3.3. Reef ensemble modeling

Predator community scenarios include variation in settlement rate,  $\rho$ , and volume constraint,  $\xi$ , over simulations. The predominant difference by far is between scenarios with and without predators. The absence of predators results in entirely different settlement and reef dynamics than the four scenarios with predators. Some differences among predator scenarios are present, and these results are shown in Supplement 4. For the remainder of results presented here, we partition the output data into two groups, one compiled across the four predator scenarios (Figs. 5, 6), and the other without predators (Figs. 7, 8).

##### 3.3.1. Scenarios with predators

Simulations of biomass, settlement habitat, and observed population demography with predators show some multi-year trends (Figs. 5, 6). The overall pattern is an initial loss of crushed shell in the first several years while the live population establishes, followed by growth and saturation of the live population, and then accumulation of valves and settlement habitat, which also stabilize several years later. Total biomass on reefs varies considerably across simulations. In some simulations, the initial shell loss is recovered through live production. The demographic structure of the population also passes through similar phases.

Live oyster biomass gradually accumulates over the first ten years of simulations (Fig. 5, second row), then stabilizes between 2003 and 2009 for lower and upper quantiles, respectively, maintaining these levels until the end of runs in 2018. This timing difference indicates that some

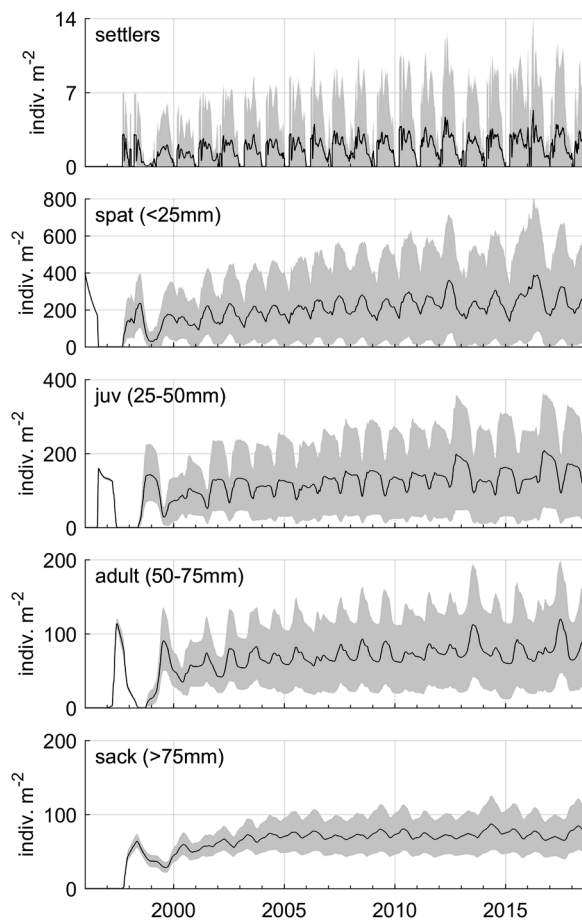


**Fig. 6.** Observed demographic size structure of the population through time (1996–2018) for scenarios with predators, summarized as density of individuals (number  $m^{-2}$ ) within four observed size classes (bottom four rows), and as density of settlers (top row). All variables are summarized as daily quantile distributions over  $\sim 1,200$  runs for each scenario (light gray bands,  $\tau = 0.1 - 0.9$ ). Black lines indicate daily means.

simulations reach volumetric capacity earlier than others. Valve biomass (third row) follows a similar pattern, but does not stabilize until approximately 2013, and shows pronounced seasonal variation. Crushed shell biomass (first row) decreases considerably in the first seven to ten years, from initial restored levels down to approximately  $4.6 \times 10^3$  kg, due to shell degradation exceeding production by the live population. From this point on, the trajectories of crushed shell diverge across simulations. Some continue along the declining trend, while others show some recovery, approaching restored levels by the end of runs. This trend is also reflected in total reef biomass (Fig. 5, bottom row), which is comprised predominantly of crushed shell, an order of magnitude higher than live oyster and valve biomass.

Settlement habitat area (Fig. 5, right column) follows similar dynamics between shell types, but with some differences across quantile ranges. Crushed shell settlement habitat (first row), declines in the initial years (1996–2002), similar to crushed biomass, but remains at similar levels until the end of the simulation, with some seasonal and annual fluctuation. Exceedance of threshold,  $\xi$  (indicated by zero values), first occurs in simulations around 2002, although this limit is not reached in all runs. Settlement habitat on live oysters (second row) initially increases on average (black line) until 2002, where it stabilizes and then fluctuates, similar to crushed shell. The upper quantile for this variable gradually increases throughout runs, although at a low rate compared to other variables. Settlement area on valves (third row) initially grows at a slower rate than live oysters, but then exceeds it in

2000, and attains much higher levels overall. Toward the end of runs, total settlement habitat on valves is approximately four times the amount on crushed shell or live oysters. Finally, settlement habitat summed together across shell types (bottom row) shows an initial dip and recovery over the first six years, as the live population is establishing. Settlement habitat is exceptionally high in 2012 and 2016.

Densities of live individuals under the predator scenario follow four approximate phases (Fig. 6). These were the initial transient dynamics of the seed stock (1996–2000), followed by increase in densities of all size classes (2000–2005), then continued increase in lower size class densities and leveling off of upper classes (2005–2012), and finally, culmination in a large recruitment year in 2012, with considerable interannual variability following it (2012–2018). During the first four years, settlement is strongly coupled to spawning, with two distinct settlement cohorts. The initial cohort of oysters stocked in 1996 reaches the sack class in 1998 (bottom row), and the first reproductive cycle is completed with the arrival of new settlers in 1997 (top row), which reaches sack size in  $\sim 2000$ . Following this time, spawning and settlement become more continuous throughout the season and cohorts become less distinguishable. Beginning in 2005, densities of the adult and sack classes remain at similar levels with noticeable spikes in 2008, 2009, and 2013, due to increased settlement in years following milder winters. These increases in larger size classes appear to be somewhat stepwise.

### 3.3.2. Scenarios with no predators

Scenarios with no predators (Figs. 7, 8) show three overall differences compared to those with predators. None of the simulations recover the initial loss of crushed shell biomass incurred from 1996 to 2003 (Fig. 7, left column), and all continue along the trajectory of decline until the end of runs in 2018. Settlement habitat is only intermittently available, at much lower levels than in scenarios with predators, and falls to zero every year for all simulations (i.e., none maintain continuous availability). Finally, individual densities are dominated by larger individuals (see sack class, Fig. 8), and settlement dynamics occur as single, pulsed events each year.

The overall temporal pattern of whole live and valve biomass (Fig. 7, second and third rows) is similar to the scenario with predators, however, these variables reach the volume limit,  $\xi$ , much earlier (whole live in 2000, and valve in 2006), and their levels relative to each other are inverted. Live biomass is consistently higher than valve and higher than levels with predators included. Valve biomass without predators does not exceed 100 kg in more than half of the simulations (Fig. 5), in contrast to the predator scenarios. The initial transient stocking period extends until approximately 2002, as indicated by the settlement habitat dynamics without predators (Fig. 7), which is four years later than with predators. Consistent annual settlement cohorts are also delayed until then (Fig. 8). Finally, densities of spat, juvenile, and adult classes are highly correlated with settlement dynamics, suggesting that the system has no buffer for variability in settlement habitat when there are no predators. Interestingly, some recruitment pulses come in regularly spaced, two-year couplets, for example in, 2002–2003 and 2009–2010.

### 3.3.3. Sensitivity analysis

The sensitivity of simulated oyster reef dynamics to the ensemble modeling assumptions are summarized in Fig. 9. Each sensitivity ensemble (columns 2–8) is compared to the original ‘base’ ensemble (column 1), by taking the mean, median, and quantiles  $\tau = 0.1, 0.9$  of the reef variables represented in Figs. 5–8, and calculating differences from equivalent base values. This analysis uses only the latter years of simulations (2015–2018) when reefs have generally reached equilibrium. Base ensemble values are given in absolute units (column 1), and all other columns list differences from the base. Colors and shading of the table indicate relative sensitivity, computed as differences divided by the standard deviation of each base ensemble variable. The four biomass variables (kg) and five individual density variables ( $\# m^{-2}$ ) are

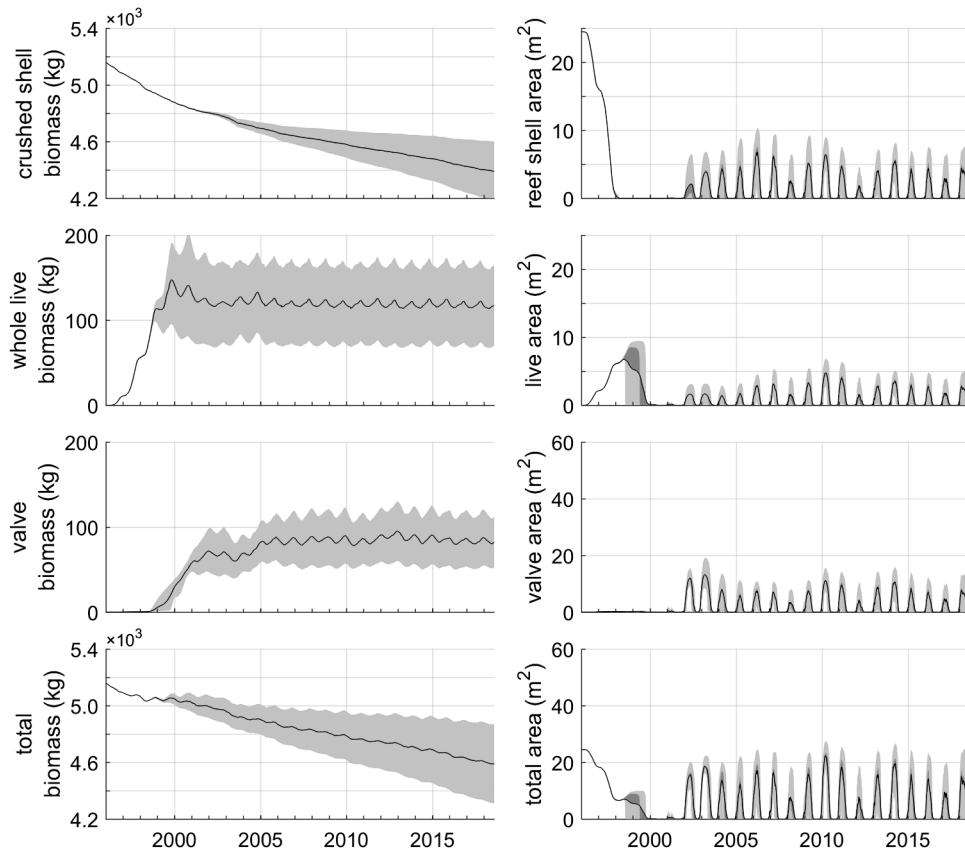


Fig. 7. Oyster reef biomass (kg) and settlement habitat ( $\text{m}^2$ ) through time (1996–2018) for scenarios with no predators. Designations are the same as Fig. 5.

generally most sensitive to changes in settlement rate,  $\rho$ , and to a lesser extent, constraint parameter,  $\xi$ . One exception is live oyster whole biomass, which is primarily sensitive to  $\xi$  and predator density. The upper quantiles of individual density are particularly sensitive to  $\rho$ . The four variables representing available settlement habitat area are mixed responses. The lower quantile ( $\tau = 0.1$ ) is most sensitive to increases in predation and parameter,  $\xi$ , both of which contribute to maintaining the live population below the volumetric limit. The mean, median, and 0.9 quantile of valve and total settlement area are most sensitive, intuitively, to the ensemble where individual valve and live exposed surface areas are assumed equal (column 8). Sensitivity of biomass and individual densities to this ensemble are moderate, but considerably less than to  $\rho$ . Note that the ratios of total valve settlement area to live for this ensemble are approximately double (1.7, 1.9, 2.0, and 2.2, for each metric, respectively), despite using the same constant. Corresponding measures for the base ensemble are 0, 4.2, 4.4, and 4.7. Interestingly, individual densities are not particularly sensitive to predator density, but are somewhat elevated at the mean and upper quantile of the terminal sack size class.

### 3.3.4. Settlement habitat availability and live population

The relationship between settlement habitat availability and the live population is shown in Fig. 10. This resembles a stock-recruitment relationship insofar as it represents settlement potential based on habitat, but does not account for recruit survival. Each light gray point in the figure indicates a single time step of simulation runs. Collectively, they summarize trends across and within simulations. Total available settlement area per unit biomass (top row), and per individual density (adult and sack class, bottom row), together represent the efficiency of the live population for generating settlement habitat under volumetric constraints, given that total surface area and volume of the population vary with population size structure. Settlement area per live biomass

(top left panel) is highest around  $\sim 150$  kg live biomass, and abruptly converges to zero above this level. This upper limit may be due to the population volume exceeding the limit,  $\xi$ , or settlement surfaces becoming completely covered, or both. Settlement area is much higher for ratios of live to valve biomass above 1 (top right panel). Lines indicating mean and median settlement area increase nonlinearly for values above 1. The relationship of settlement area to adult density (bottom left) is dome-shaped with maxima around 200 individuals  $\text{m}^{-2}$ , while the same relationship for the sack class (bottom right) resembles a sigmoidal or other saturating curve, which increases between 50 and 100 individuals  $\text{m}^{-2}$ . When sack densities are high, high levels of settlement habitat are usually maintained. In contrast, settlement habitat falls to zero in nearly all simulations when adult densities are high, as indicated by the divergence between the mean and median above 300 individuals  $\text{m}^{-2}$ . This suggests that the exposed surface areas, or volume of the population relative to  $\xi$ , are saturated by many smaller individuals, which taken together are less efficient at producing and exposing shell for settlement than larger individuals.

## 4. Discussion

We developed an individual-based model of oyster reef mechanics to simulate interacting effects of metabolism, growth, mortality, predation, and environmental conditions on the engineering and maintenance of reef structure by oyster populations. The modeled reef functions as a complex adaptive system (Railsback 2001), with interrelated dynamics between the live population and reef shell, across multiple scales of individuals, population, and physical habitat. Together, these determine reef self-organization. Key results of this study include new insights into the role of predators and mortality on the rates of shell production and turnover by the oyster reef system, an important mechanism for generating settlement habitat in this model. These include the overall

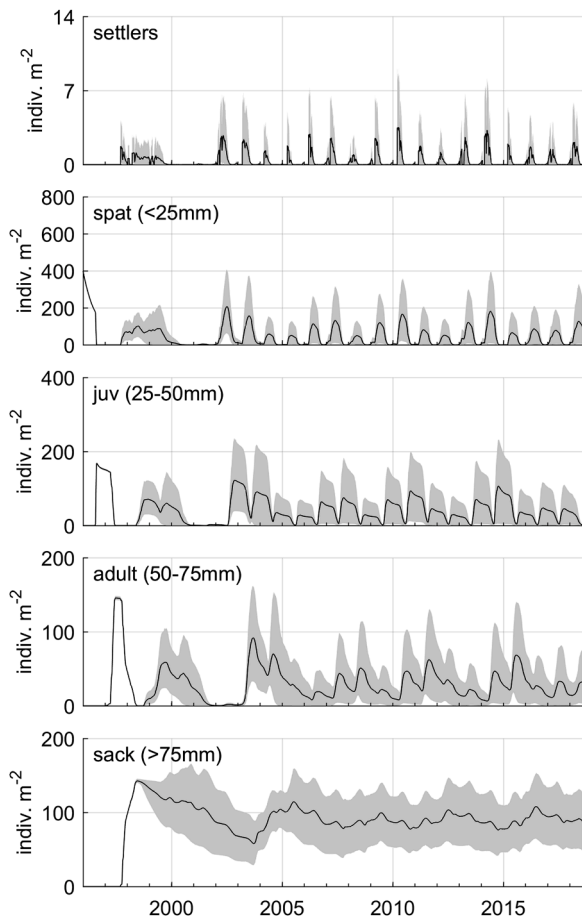


Fig. 8. Demographic size structure of the population through time (1996–2018) for scenarios with no predators. Designations are the same as Fig. 6.

amount of shell produced by the population, the size of individual shells and their longevity on the reef, and the transfer of shell to become settlement habitat. All three of these aspects are determined by oyster growth and size at the individual level, the overall population size and demographic size structure, and mortality, imposed externally through predation and other sources. Results of this study represent new hypotheses and predictions for how internal proximal drivers of the oyster population interact with external factors to determine reef self-organization. Our oyster reef model can be broadly adapted to test these and other hypotheses and predictions in field studies. It requires only three input data sets (salinity, temperature, and food source) and reasonable assumptions on predator dynamics, mortality, shell degradation, and settlement, which can be updated when better estimates become available.

Three phases of reef dynamics that are robust across simulations are identified in the ensemble modeling: (1) initial shell loss concurrent with live population growth, (2) saturation of the live population, and (3) saturation of settlement habitat. The timing of these phases varies with levels of predation activity, particularly the length of time required for the population to establish and overcome the initial transient stocking dynamics. Simulated reefs vary considerably in their ability to maintain sufficient shell biomass to support accretion, and continuous availability of settlement habitat. Importantly, accretion and settlement are linked mechanically through shell production. In all simulations without predators, reefs fall into decline, and demonstrate highly correlated spawning and settlement due to intermittent settlement habitat availability. The only mortality factors for this scenario are natural mortality, burial, and terminal age, suggesting that larger-sized

oysters obstruct settlement by suppressing the exposure of valves. Simulations with predators show varying degrees of settlement habitat availability. More than half provide continuous habitat for at least a large portion of simulation runs. These results suggest that strongly correlated spawning stock-recruitment cycles may indicate instability through discontinuous habitat availability and insufficient recruitment to sustain the population. In contrast, the somewhat decoupled, continuous settlement habitat associated with more complex population size structures may mediate reef stability (Figs. 5, 6, 10; also Powell and Klinck 2007, Kuykendall et al., 2015). We urge caution when interpreting the role of predators in this study. Our focus is on how oysters have evolved to interact with predators in a way that supports their long-term persistence, and not identify levels that drive the population to extinction.

In developing this IBM, we draw from several previous modeling studies. Powell et al. (1992) and Hofmann et al. (1994) developed a comprehensive suite of models which pioneered the examination of population level processes that emerge from individual physiology. We follow a similar approach, but replace their empirically-derived filtration rates with the more mechanistic DEB approach. Powell et al. (2006) and Powell and Klinck (2007) developed mathematical equations for deriving rates of shell persistence on reefs, Wilberg et al. (2013) developed a system of equations representing coupled dynamics of oyster and shell habitat at the population level, and Soniat et al. (2012) developed a mathematical model which specified objectives for maintaining net balance of shell. We incorporate these concepts of shell persistence, net balance, and coupled dynamics into a single platform, additionally including properties of shell surface area, which requires building up dynamics mechanistically from individuals, through shell growth, mortality, and biomass accumulation. We also allow for age and size to be somewhat independent, insofar as they determine cohort dynamics. Moore et al. (2016) found this distinction important in their integral projection model, although it is often not included in matrix-based modeling. By explicitly tracking valves with individual variation, we can examine the complex shell surfaces available for settlement with respect to population size and demographic size structure (Fig. 10). Our results showing that settlement area increases with both of these measures agree with those of Schulte et al. (2009) for restored high relief reefs (see their Fig. 4), which were considerably more successful than low relief. Interestingly, that study found a similar quadratic relationship between recruits and the adult population.

The results of our study are contingent on several limitations of the model, assumed for the present application. First, mortality is applied generally at low levels. We acknowledge that in real reefs, mortality is a key agent for population decline, particularly when stressors act in combination, such as disease (Ford et al., 2006), predation (Grabowski 2004), depletion of shell resources (Camp et al. 2015, Colden et al., 2017, Frederick et al., 2016), limitation in food supply, sedimentation (Colden et al., 2017, Jordan-Cooley et al., 2011), and extreme and episodic environmental conditions (La Peyre et al. 2016, Lowe et al., 2017, Puckett and Eggleston 2012). Our focus here is to examine how mortality facilitates availability of settlement habitat, thus we do not address this complexity of factors. We model predation only as intermittent events, and not as persistent and overwhelming predator outbreaks. Similarly, we describe sedimentation implicitly as a probability of burial, and keep the natural mortality function constant over time, to simulate low levels of these mortalities which provide background regulation of the live oyster population. Material contribution of sedimentation is not examined here, since this is highly variable across watersheds and time (Isphording and Imsand 1991, Liu and Huang 2009), and research suggests that mortality from sedimentation only occurs when it exceeds ~30 mm total, and is maintained for over 28 days (i.e., Colden et al., 2017). We do not allow any individuals to expire through loss of energy reserves in the DEB routine, which only occurs infrequently at very young ages (< 2 weeks). Finally, we do not include anthropogenic harvest, although we acknowledge that it can strongly

		base	pred ↓	pred ↑	$\rho$ ↓	$\rho$ ↑	$\xi$ ↓	$\xi$ ↑	valve=live	
shell (kg)	$\tau=0.1$	4389.30	-59.88	22.87	-270.48	165.29	-257.83	137.31	-68.67	sensitivity 
	med	4628.80	-12.19	-16.55	-278.32	269.39	-117.04	123.38	-124.88	
	mean	4639.20	-11	-34.74	-292.71	232.81	-149.05	112.90	-127.12	
	$\tau=0.9$	4905.35	26.59	-109.79	-338.49	240.76	-89.21	61.19	-186.26	
valve (kg)	$\tau=0.1$	71.52	-6.88	6.05	-28.47	15.15	-37.38	31.18	-7.38	
	med	115.82	-1.56	-5.58	-36.54	25.74	-23.42	22.24	-19.02	
	mean	116.70	-1.79	-6.98	-36.44	22.56	-26.29	22.80	-18.45	
	$\tau=0.9$	162.29	2.97	-21.32	-43.62	25.60	-20.61	15.96	-29.06	
live whole (kg)	$\tau=0.1$	65.76	2.42	-0.06	1.51	0.94	-25.20	27.14	2.18	
	med	103.82	6.68	-12.84	-7.18	6.49	-21.19	16.69	-4.30	
	mean	103.18	8.47	-12.75	-8.20	5.48	-21.23	18.81	-4.23	
	$\tau=0.9$	138.43	17.26	-25.06	-20.07	9.65	-17.26	13.82	-11.87	
all shell (kg)	$\tau=0.1$	4510.25	-67.61	35.33	-286.93	178.90	-315.25	194.30	-70.55	
	med	4816.68	-5.88	-30.38	-324.10	306.62	-153.03	156.33	-145.61	
	mean	4827.61	-6.73	-50.64	-334.79	259.26	-189.99	148.67	-148.51	
	$\tau=0.9$	5156.79	43.48	-147.85	-392.19	271.38	-118.01	84.47	-224.06	
avail shell (m <sup>2</sup> )	$\tau=0.1$	0	0	4.01	1.42	0	0	3.90	0.53	
	med	7.12	-2.06	1.40	0.99	-0.88	-0.64	-0.02	-1.56	
	mean	6.12	-1.87	1.70	1.07	-0.89	-1.08	0.53	-1.07	
	$\tau=0.9$	9.28	-1.03	0.84	0.38	-0.49	0.11	-0.38	-1.91	
avail valve (m <sup>2</sup> )	$\tau=0.1$	0	0	8.39	1.72	0	0	14.03	0.54	
	med	24.10	-10.46	2.99	-8.50	3.94	-10.53	7.47	-16.05	
	mean	22.12	-7.52	3.05	-6.78	2.82	-7.57	7.96	-14.55	
	$\tau=0.9$	39.03	-6.21	-2.30	-11.40	6.87	-5.99	4.58	-26.81	
avail live (m <sup>2</sup> )	$\tau=0.1$	0	0	2.09	0.65	0	0	3.66	0.32	
	med	5.77	-2.02	0.20	-0.76	0.28	-2.31	1.48	-1.42	
	mean	5.06	-1.38	0.39	-0.51	0.13	-1.70	1.74	-1.22	
	$\tau=0.9$	8.38	-0.47	-0.82	-1.55	0.81	-1.19	0.93	-2.82	
avail all (m <sup>2</sup> )	$\tau=0.1$	0	0	14.94	3.98	0	0	22.42	1.43	
	med	38.33	-14.65	3.87	-8.96	3.66	-13.88	8.29	-19.63	
	mean	33.30	-10.77	5.14	-6.21	2.06	-10.35	10.24	-16.83	
	$\tau=0.9$	54.33	-6.96	-2.41	-11.86	6.96	-6.31	4.63	-31.21	
settlers (# m <sup>-2</sup> )	$\tau=0.1$	0	0	0	0	0	0	0	0	
	med	0	0	0	0	0	0	0	0	
	mean	2.23	-0.48	0.13	-1.36	2.18	-0.67	0.65	-0.94	
	$\tau=0.9$	7.15	-1.70	0.50	-4.50	7.90	-2.30	2.15	-3.10	
spat (# m <sup>-2</sup> )	$\tau=0.1$	23.70	-10.35	6.25	-13.60	-11.55	-21.60	31.55	4.25	
	med	192.10	-56.80	17.45	-116.95	127.95	-83	68.60	-65.90	
	mean	245.78	-47.40	11.24	-137.99	166.25	-71.47	64.95	-88.23	
	$\tau=0.9$	537.65	-66.85	7.85	-286.30	383.35	-93	90.60	-204.90	
juv (# m <sup>-2</sup> )	$\tau=0.1$	31.55	-10.50	6.05	-20.35	-0.95	-23.05	24.30	-2.20	
	med	125.15	-24.60	5.30	-68.65	54.70	-44.30	35.65	-38.25	
	mean	136.30	-16.69	0.89	-66.09	44.67	-35.44	30.17	-37.28	
	$\tau=0.9$	256.30	-9.25	-11.80	-105.75	63.35	-31.95	27.40	-69.80	
adult (# m <sup>-2</sup> )	$\tau=0.1$	26	-6.45	3.70	-14.85	3.25	-17.10	14.10	-2.15	
	med	69.10	-9.30	-0.25	-30.35	21.70	-21.50	17.95	-15.50	
	mean	74.38	-5.99	-2.02	-30.59	18.82	-19.16	16.42	-15.95	
	$\tau=0.9$	130	-0.70	-10.65	-47	28.85	-17.65	16	-30.20	
sack (# m <sup>-2</sup> )	$\tau=0.1$	45.30	3.70	-2.90	1.15	-0.75	-14.20	13.65	1.65	
	med	68.75	8	-9.95	-5.10	3.30	-12.55	11	-2.15	
	mean	70.15	8.75	-10.11	-5.70	3.33	-12.92	11.41	-2.58	
	$\tau=0.9$	96.75	15	-17.70	-13.75	7.55	-11.90	9.85	-7.65	

Fig. 9. Results of sensitivity analysis. Seven additional sensitivity ensembles (columns 2–8) are compared to base results (column 1), for 13 key reef variables (rows), summarized as the mean, median, and two quantile levels ( $\tau = 0.1, 0.9$ ). Base values are given in absolute units, and all others are listed as net differences from base. Color indicates relative sensitivity, scaled by standard deviation of each base variable. (For interpretation of the references to colour in this figure legend, the reader is referred to the web version of this article.)

determine oyster reef persistence (Camp et al. 2015).

Modeling a complete oyster reef system, including whole organisms and shell, requires integrating information across field (Kuykendall et al., 2015, Powell et al., 2006, Powell and Klinck 2007), and modeling studies (Hofmann et al., 1994, Lavaud et al., 2017, W.E. Pine et al. 2015, Powell et al., 1992), that span several populations in the Atlantic and Gulf of Mexico coasts (USA). We acknowledge that these populations may differ in genetics, phenotype, systems dynamics, and other traits that could alter modeled outcomes. Our goal here is to develop a holistic model that sets testable predictions for any population of interest (Nichols and Williams 2006), and not necessarily to describe a specific population. We focus on developing a model based on mechanical principles that are common among populations (e.g., energy flux, shell surface area), and whenever possible, minimize assumptions of empirically-derived parameters that may be population-specific. For

example, our modeled shell degradation is based on a population-level annual rate determined for a Delaware Bay (USA) population (Powell and Klinck 2007). We generalize this rate with respect to individual shell mechanics by modeling degradation at the daily scale as a function of individual shell biomass, which is determined by individual growth in the DEB model. These individual degradation dynamics then combine in the model at the population level, approximating the annual rates of Powell & Klinck (2007).

Several physical constraints on reef geomorphology are applied in this study which may be more variable in real reef systems. Reef morphological dynamics are governed primarily by change in total volume of the assumed trapezoidal-shaped reef. The base horizontal dimensions,  $x1, x2$  (Fig. 2), are fixed across simulations, the constraint on live oyster volume,  $\xi$ , is fixed during runs, and reef height,  $h$ , is assumed static across the spatial extent of the reef. In real reefs, these

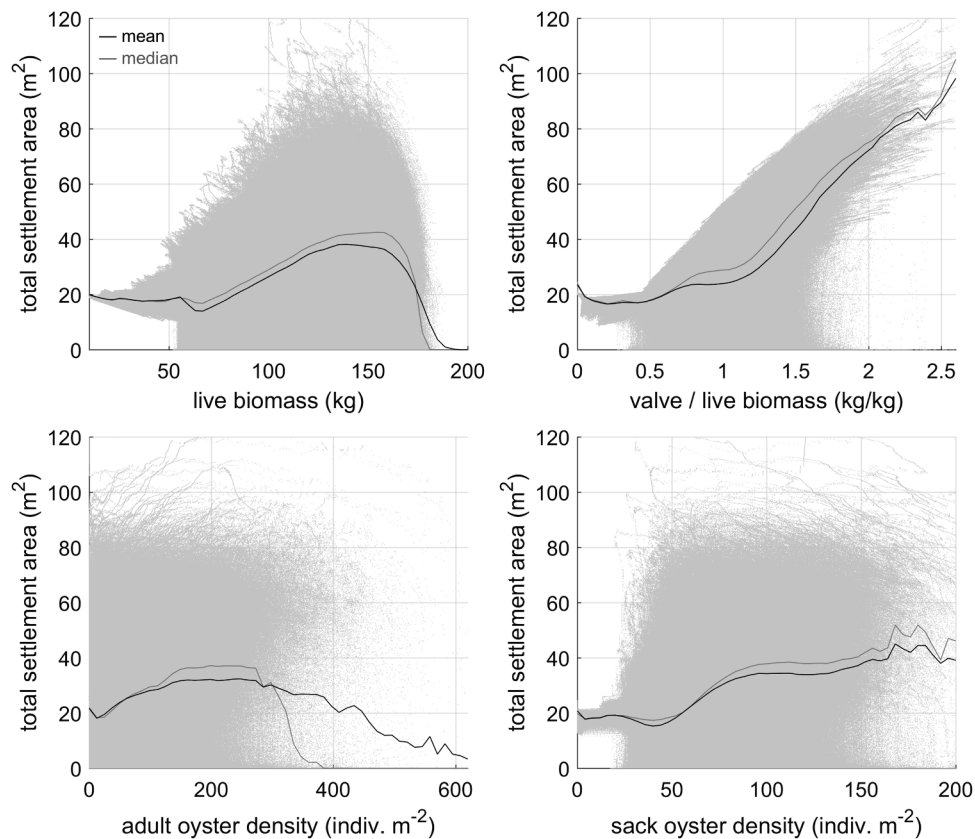


**Fig. 10.** Total settlement habitat area ( $\text{m}^2$ ) compared to measures of biomass and individual density (number  $\text{m}^{-2}$ ) for scenarios with predators only. Light gray dots indicate simulation data over entire simulation runs. Black and gray lines indicate mean and median, respectively. Top and bottom rows represent efficiency of the system for generating settlement habitat relative to population size (per unit biomass), and relative to size structure (number of larger individuals), respectively.

vary spatiotemporally as reef morphology interacts with dynamic landscape conditions, and spatial heterogeneity in reef composition is likely a key property contributing to reef resilience. This has been demonstrated for mussel beds (Liu et al., 2014) and coral reefs (Toth et al., 2019), but remains relatively unexamined for oyster reefs. Allowing for spatial expansion of shell habitat in future modeling studies may reduce the cumulative effect of the constraints imposed here. For example, the assumption of fixed base dimensions in our model precludes horizontal expansion, which taken together with  $\xi$ , imposes both vertical and horizontal limitations which may have facilitated the stepwise increases in individual density observed in later years of simulations. Nonetheless, it is reasonable to assume that both types of constraints could be present in high wave energy or hydrodynamic environments. It is also possible that  $\xi$  is dynamic on real reefs, considering that changes in reef elevation or shell drag can attenuate wave energy (Allen and Webb 2011). Threshold effects of reef elevation are also possible, such as found by Colden et al., (2017), however, we do not include these here. Finally, real reefs take many complex forms, including elongated, fringing, winding, or mounding bars, which are determined largely by local bathymetry and hydrodynamics. We do not assume any specific landscape effects in this study, although factors such as reef elevation and location with respect to the tidal prism are known to impact growth and survival rates of oysters (Dame 1971, 1972). Despite these assumptions, we believe that the present model achieves a reasonable compromise between simplification and complexity of the complicated reef-building system, and sets appropriate baselines for more targeted studies.

Our oyster reef model can be applied to support restoration decision making. Oyster reefs are gaining increasing attention for their potential value for supporting shoreline stabilization, for example, through wave attenuation (Allen and Webb 2011, Currin et al., 2010, Piazza et al.,

2005, Scyphers et al., 2011), and for their self-maintaining ‘resilience’ properties (Bahr and Lanier 1981). These ecosystem services could greatly reduce investment and maintenance costs (Allen and Webb 2011) and greatly increase overall restoration value, considering the ability of populations to stabilize themselves over large fluctuations in the physical environment (e.g., drought, flooding, sea level change), and their secondary benefits for ecosystems (Coen et al., 2007, Grabowski et al., 2012, Lipcius et al., 2019). However, the history of oyster reef restoration shows considerable uncertainty. For example, La Peyre et al. (2014) found that ~27% of northern Gulf of Mexico restorations failed to maintain targets for live oyster density ( $> 0$  oysters  $\text{m}^{-2}$ ), and ~18% lacked elevational relief ( $> 0$  L substrate  $\text{m}^{-2}$ ). Such failures could be due to the inability of the reef to develop self-organizing, resilience properties. Therefore, it is critical to know which conditions may contribute to the establishment of such resilience, so that the correct information can be conveyed to restoration practitioners.

One of the chief concerns for restoration decision making is risk of investment losses due to various sources of uncertainty. In this study, we attempted to explain some of the uncertainty associated with reef ‘resilience’, which is often extolled but poorly described. In simulating single restorations, we represented a management objective of investing in habitat and stock in the short term to promote long-term population self-maintenance, which could considerably reduce overall costs. Our modeling shows some lags in the response of the reef to restorations, which extends from five to eight years, suggesting that return on investment may not become evident until later than expected. During this time, reefs may be particularly vulnerable as they recover from initial transient conditions. We acknowledge that modeled outcomes show considerable variability across simulations. Our goal for this study is not to identify exact conditions that optimize restoration investment, but to identify robust trends across simulations that improve scientific

understanding of key mechanistic processes, and thus offer insight into how restorations may be valued through time. In this way, predictions made by the reef model can support future studies in both ecology and decision analysis.

## 5. Conclusion

This individual-based model advances oyster modeling by representing reef dynamics as three-dimensional mechanical processes. Internal drivers and external factors interact to determine reef self-organization. The model tracks these dynamics as they transfer across individual, population, and reef scales. Shell habitat functions as both material supporting reef geomorphology and as substrate regulating larval settlement. Results from the model show that the reef system maintains organization through efficient generation of settlement habitat, measured with respect to live biomass and density of larger sized individuals. This suggests that individual production, population size structure, and physical environmental constraints all contribute to reef self-organization. Results also show important multi-year lags in reef dynamics following restoration, suggesting that a period of five to eight years may be necessary for the reef to recover and equilibrate, before it maintains efficient production. This modeling framework could be applied to support restoration decision making, and to examine other self-organizing systems, such as coral or sponge reefs.

## Credit author statement

**Simeon Yurek**, lead developer and corresponding author, **Mitchell J. Eaton**: conceptualization, methodology, writing – original draft, **Romain Lavaud**, conceptualization, methodology, writing – original draft, software, validation, **R. Wilson Laney**: conceptualization, investigation, writing – review and editing, **Donald L. DeAngelis**: writing – original draft, **William E. Pine III**: conceptualization, funding acquisition, **Megan La Peyre**: conceptualization, writing – review and editing, **Julien Martin**: conceptualization, writing – review and editing, project administration, **Peter Frederick**: conceptualization, **Hongqing Wang**: validation, writing – review and editing, **Michael R. Lowe**: conceptualization, writing – review and editing, **Fred Johnson**: conceptualization, **Edward V. Camp**: conceptualization, **Rua Mordecia**: conceptualization, project administration, supervision, writing – review and editing, funding acquisition

## Declaration of Competing Interest

The authors declare that they have no known competing financial interests or personal relationships that could have appeared to influence the work reported in this paper.

## Acknowledgments

We thank Donald Schoolmaster, Jr. and six anonymous reviewers for generously donating their time to review this publication. We especially thank Baruch Institute for sharing data, North Carolina State University for use of high performance computing facilities, and the North Carolina Wildlife Resources Commission for use of facilities. This work was supported by the U.S. Fish and Wildlife Service in collaboration with the U.S. Geological Survey, supporting Southeast Conservation Adaptation Strategy (<http://secassoutheast.org>), and by the office of the Senior Vice-President of the Institute of Food and Agricultural Sciences at the University of Florida (UF/IFAS), the Department of Wildlife Ecology and Conservation, and Nature Coast Biological Station. Any use of trade, firm, or product names is for descriptive purposes only and does not imply endorsement by the U.S. Government.

## Supplementary materials

Supplementary material associated with this article can be found, in the online version, at [doi:10.1016/j.ecolmodel.2020.109389](https://doi.org/10.1016/j.ecolmodel.2020.109389).

## References

- Allen, R.J., Webb, B.M., 2011. Determination of wave transmission coefficients for oyster shell bag breakwaters. *Coast. Eng. Pract.* 2011, 684–697.
- Arkema, K.K., Guannel, G., Verutes, G., Wood, S.A., Guerry, A., Ruckelshaus, M., Kareiva, P., Lacayo, M., Silver, J.M., 2013. Coastal habitats shield people and property from sea-level rise and storms. *Nat. Clim. Chang.* 3 (10), 913.
- Bahr, L.M., Lanier, W.P., 1981. The Ecology of Intertidal Oyster Reefs of the South Atlantic coast: a Community profile (No. 81/15). U.S. Fish and Wildlife Service.
- Bartol, I.K., Mann, R., 1997. Small-scale settlement patterns of the oyster *Crassostrea virginica* on a constructed intertidal reef. *Bull. Mar. Sci.* 61 (3), 881–897.
- Beddington, J.R., 1975. Mutual interference between parasites or predators and its effect on searching efficiency. *J. Anim. Ecol.* 331–340.
- Bignell, D.E., Roisin, Y., Lo, N. (Eds.), 2010. *Biology of termites: a Modern Synthesis*. Springer Science & Business Media.
- Brown, K.M., Richardson, T.D., 1988. Foraging ecology of the southern oyster drill *Thais haemastoma* (Gray): constraints on prey choice. *J. Exp. Mar. Biol. Ecol.* 114 (2–3), 123–141.
- Brown, K.M., George, G.J., Peterson, G.W., Thompson, B.A., Cowan, J.H., 2008. Oyster predation by black drum varies spatially and seasonally. *Estuaries and Coasts* 31 (3), 597–604.
- Butler, P.A., 1985. Synoptic review of the literature on the southern oyster drill *Thais haemastoma floridae*. NOAA Technical Report NMFS 35. U.S. Department of Commerce.
- Camazine, S., Deneubourg, J.-L., Franks, N.R., Sneyd, J., Theraulaz, G., Bonabeau, E., 2001. *Self-organization in Biological Systems*. Princeton Studies in Complexity. Princeton University Press, Princeton, NJ.
- Pine III, Camp, E., Havens, W., Kane, K., Walters, A., Irani, C., Lindsey, A., T., Morris Jr., J., 2015. Collapse of a historic oyster fishery: diagnosing causes and identifying paths toward increased resilience. *Ecol. Soc.* 20 (3).
- Coen, L.D., Brumbaugh, R.D., Bushek, D., Grizzle, R., Luckenbach, M.W., Posey, M.H., Powers, S.P., Tolley, S.G., 2007. Ecosystem services related to oyster restoration. *Mar. Ecol. Prog. Ser.* 341, 303–307.
- Colden, A.M., Latour, R.J., Lipcius, R.N., 2017. Reef height drives threshold dynamics of restored oyster reefs. *Mar. Ecol. Prog. Ser.* 582, 1–13.
- Curran, C.A., Chappell, W.S. and Deaton, A., 2010. Developing Alternative Shoreline Armoring strategies: the Living Shoreline Approach in North Carolina.
- Dame, R.F., 1971. The Ecological Energies of growth, Respiration and Assimilation in the Intertidal American oyster, *Crassostrea virginica* (Gmelin). Ph. D. Thesis. University of South Carolina, <http://libcat.csd.sc.edu/record=b1435865--S1> (Accessed: 17 July 2019).
- Dame, R.F., 1972. The ecological energies of growth, respiration and assimilation in the intertidal American oyster *Crassostrea virginica*. *Mar. Biol.* 17 (3), 243–250.
- Dame, R., Bushek, D., Allen, D., Edwards, D., Lewitus, A., Koepfler, E., Kjerfve, B., Gregory, L., 2000. CREEK Project: RUI: the Role of Oyster Reefs in the Structure and Function of Tidal Creeks. Originators: Coastal Carolina University and Belle W. Baruch Institute for Marine and Coastal Sciences, University of South Carolina, Georgetown, SC.
- Day Jr., J.W., Kemp, W.M., Yanez-Arancibia, A., Crump, B.C., 2012. In: Day Jr., Kemp, Yanez-Arancibia, Crump (Eds.). Wiley-Blackwell, New York, NY USA. ISBN: 978-0-471-75567-8.
- DeAngelis, D.L., Goldstein, R.A., O'Neill, R.V., 1975. A model for tropic interaction. *Ecology* 56 (4), 881–892.
- Dekshenieks, M.M., Hofmann, E.E., Klinck, J.M., Powell, E.N., 2000. Quantifying the effects of environmental change on an oyster population: a modeling study. *Estuaries* 23 (5), 593.
- Eggleston, D.B., 1990. Behavioural mechanisms underlying variable functional responses of blue crabs, *Callinectes sapidus* feeding on juvenile oysters, *Crassostrea virginica*. *J. Anim. Ecol.* 615–630.
- Ford, S.E., Cummings, M.J., Powell, E.N., 2006. Estimating mortality in natural assemblages of oysters. *Estuaries and Coasts* 29 (3), 361–374.
- Frederick, P., Vitale, N., Pine, B., Seavey, J., Sturmer, L., 2016. Reversing a rapid decline in oyster reefs: effects of durable substrate on oyster populations, elevations, and aquatic bird community composition. *J. Shellfish Res.* 35 (2), 359–368.
- Gårdmark, A., Lindegren, M., Neuenfeldt, S., Blenckner, T., Heikinheimo, O., Müller-Karulis, B., Niiranen, S., Tomczak, M.T., Aro, E., Wikström, A., Möllmann, C., 2013. Biological ensemble modeling to evaluate potential futures of living marine resources. *Ecol. Appl.* 23 (4), 742–754.
- Grabowski, J.H., 2004. Habitat complexity disrupts predator–prey interactions but not the trophic cascade on oyster reefs. *Ecology* 85 (4), 995–1004.
- Grabowski, J.H., Hughes, A.R., Kimbro, D.L., 2008. Habitat complexity influences cascading effects of multiple predators. *Ecology* 89 (12), 3413–3422.
- Grabowski, J.H., Brumbaugh, R.D., Conrad, R.F., Keeler, A.G., Opaluch, J.J., Peterson, C. H., Piehler, M.F., Powers, S.P., Smyth, A.R., 2012. Economic valuation of ecosystem services provided by oyster reefs. *Bioscience* 62 (10), 900–909.
- Grimm, V., Railsback, S.F., 2005. *Individual-based Modeling and Ecology*. Princeton university press.
- Grimm, V., Berger, U., Bastiansen, F., Eliassen, S., Ginot, V., Giske, J., Goss-Custard, J., Grand, T., Heinz, S.K., Huse, G., Huth, A., 2006. A standard protocol for describing individual-based and agent-based models. *Ecol. Modell.* 198 (1–2), 115–126.

- Grimm, V., Berger, U., DeAngelis, D.L., Polhill, J.G., Giske, J., Railsback, S.F., 2010. The ODD protocol: a review and first update. *Ecol. Modell.* 221 (23), 2760–2768.
- Haller-Bull, V., Rovenskaya, E., 2019. Optimizing functional groups in ecosystem models: case study of the Great Barrier Reef. *Ecol. Modell.* 411, 108806.
- Harding, J.M., Mann, R., Southworth, M.J., 2008. Shell length-at-age relationships in James River, Virginia, oysters (*Crassostrea virginica*) collected four centuries apart. *J. Shellfish Res.* 27 (5), 1109–1115.
- Hesterberg, S.G., Duckett, C.C., Salewski, E.A., Bell, S.S., 2017. Three-dimensional interstitial space mediates predator foraging success in different spatial arrangements. *Ecology* 98 (4), 1153–1162.
- Hofmann, E.E., Klinck, J.M., Powell, E.N., Boyles, S., Ellis, M., 1994. Modeling oyster populations II. Adult size and reproductive effort. *J. Shellfish Res.* 13 (1).
- Holling, C.S., 1959. Some characteristics of simple types of predation and parasitism. *Can. Entomol.* 91 (7), 385–398.
- Huth, A., Wissel, C., 1992. The simulation of the movement of fish schools. *J. Theor. Biol.* 156 (3), 365–385.
- Ishphording, W.C., Imsand, F.D., 1991. Cyclonic events and sedimentation in the Gulf of Mexico. *Coastal Sediments. ASCE*, pp. 1122–1136.
- Jeltsch, F., Milton, S.J., Dean, W.R.J., Van Rooyen, N., Moloney, K.A., 1998. Modelling the impact of small-scale heterogeneities on tree–grass coexistence in semi-arid savannas. *J. Ecol.* 86 (5), 780–793.
- Jordan-Cooley, W.C., Lipcius, R.N., Shaw, L.B., Shen, J., Shi, J., 2011. Bistability in a differential equation model of oyster reef height and sediment accumulation. *J. Theor. Biol.* 289, 1–11.
- Kennedy, V.S., Shaw, K.S., Newell, R.I., 2009. Discriminatory predation by three invertebrates on eastern oysters (*Crassostrea virginica*) compared with non-native Sumineo oysters (*C. ariakensis*). *Invert. Biol.* 128 (1), 16–25.
- Klausmeier, C.A., 1999. Regular and irregular patterns in semiarid vegetation. *Science* 284 (5421), 1826–1828.
- Kooijman, S.A.L.M., 2010. *Dynamic Energy Budget Theory for Metabolic Organization*. University Press, Cambridge, UK, p. 532 third edition.
- Kuykendall, K.M., Moreno, P., Powell, E.N., Soniat, T.M., Colley, S., Mann, R., Munroe, D.M., 2015. The exposed surface area to volume ratio: is shell more efficient than limestone in promoting oyster recruitment? *J. Shellfish Res.* 34 (2), 217–225.
- La Peyre, M., Furlong, J., Brown, L.A., Piazza, B.P., Brown, K., 2014. Oyster reef restoration in the northern Gulf of Mexico: extent, methods and outcomes. *Ocean Coast. Manag.* 89, 20–28.
- La Peyre, M.K., Geaghan, J., Decossas, G., Peyre, J.F.L., 2016. Analysis of environmental factors influencing salinity patterns, oyster growth, and mortality in Lower Breton Sound Estuary, Louisiana, using 20 years of data. *J. Coast. Res.* 32 (3), 519–530.
- Lavaud, R., La Peyre, M.K., Casas, S.M., Bacher, C., La Peyre, J.F., 2017. Integrating the effects of salinity on the physiology of the eastern oyster, *Crassostrea virginica*, in the northern Gulf of Mexico through a Dynamic Energy Budget model. *Ecol. Modell.* 363, 221–233.
- Lenihan, H.S., 1999. Physical–biological coupling on oyster reefs: how habitat structure influences individual performance. *Ecol. Monogr.* 69 (3), 251–275.
- Levin, S.A., 1992. The problem of pattern and scale in ecology: the Robert H. MacArthur award lecture. *Ecology* 73 (6), 1943–1967.
- Lillis, A., Bohnenstiehl, D.R., Eggleston, D.B., 2015. Soundscape manipulation enhances larval recruitment of a reef-building mollusk. *PeerJ* 3, e999.
- Lipcius, R.N., Eggleston, D.B., Fodrie, F.J., van der Meer, J., Rose, K.A., Vasconcelos, R.P., van de Wolfshaar, K.E., 2019. Modeling Quantitative Value of Habitats for Marine and Estuarine Populations. *Front. Mar. Sci.* 6, 280.
- Liu, Q.X., Herman, P.M., Mooij, W.M., Huisman, J., Scheffer, M., Olf, H., Van De Koppel, J., 2014. Pattern formation at multiple spatial scales drives the resilience of mussel bed ecosystems. *Nat. Commun.* 5, 5234.
- Liu, X., Huang, W., 2009. Modeling sediment resuspension and transport induced by storm wind in Apalachicola Bay, USA. *Environ. Modell. Softw.* 24 (11), 1302–1313.
- Lord, J.P., 2014. *Effect of Temperature Changes on Competitive and Predator-Prey Interactions in Coastal Epi-Benthic Communities*. <https://opencommons.uconn.edu/cgi/viewcontent.cgi?referer=https://scholar.google.com/&httpsredir=1&article=6692&context=dissertations>.
- Lorenzen, K., 2000. Allometry of natural mortality as a basis for assessing optimal release size in fish-stocking programmes. *Can. J. Fish. Aqua. Sci.* 57 (12), 2374–2381.
- Lowe, M.R., Sehlinger, T., Soniat, T.M., Peyre, M.K.L., 2017. Interactive effects of water temperature and salinity on growth and mortality of eastern oysters, *Crassostrea virginica*: a meta-analysis using 40 years of monitoring data. *J. Shellfish Res.* 36 (3), 683–697.
- Menzel, W.R., Nichy, F.E., 1958. Studies of the distribution and feeding habits of some oyster predators in Alligator Harbor, Florida. *Bull. Mar. Sci.* 8 (2), 125–145.
- Moore, J.L., Lipcius, R.N., Puckett, B., Schreiber, S.J., 2016. The demographic consequences of growing older and bigger in oyster populations. *Ecol. Appl.* 26 (7), 2206–2217.
- O'Connor, N.E., Grabowski, J.H., Ladwig, L.M., Bruno, J.F., 2008. Simulated predator extinctions: predator identity affects survival and recruitment of oysters. *Ecology* 89 (2), 428–438.
- Nestlerode, J.A., Luckenbach, M.W., O'Beirn, F.X., 2007. Settlement and survival of the oyster *Crassostrea virginica* on created oyster reef habitats in Chesapeake Bay. *Restor. Ecol.* 15 (2), 273–283.
- Newell, R.I., Kennedy, V.S., Shaw, K.S., 2007. Comparative vulnerability to predators, and induced defense responses, of eastern oysters *Crassostrea virginica* and non-native *Crassostrea ariakensis* oysters in Chesapeake Bay. *Mar. Biol.* 152 (2), 449–460.
- Nichols, J.D., Williams, B.K., 2006. Monitoring for conservation. *Trends Ecol. Evol.* (Amst.) 21 (12), 668–673.
- Piazza, B.P., Banks, P.D., La Peyre, M.K., 2005. The potential for created oyster shell reefs as a sustainable shoreline protection strategy in Louisiana. *Restor. Ecol.* 13 (3), 499–506.
- Pine III, W.E., Walters, C.J., Camp, E.V., Bouchillon, R., Ahrens, R., Sturmer, L., Berrigan, M.E., 2015b. The curious case of eastern oyster *Crassostrea virginica* stock status in Apalachicola Bay, Florida. *Ecol. Soc.* 20 (3).
- Powell, E.N., Hofmann, E.E., Klinck, J.M. and Ray, S.M., 1992. Modeling oyster populations: I. A commentary on filtration rate. Is faster always better?. *J. Shellfish Res.*
- Powell, E.N., Klinck, J.M., Hofmann, E.E. and Ray, S.M., 1994. Modeling oyster populations. IV: rates of mortality, population crashes and management. *Fish. Bull.*
- Powell, E.N., Kraeuter, J.N., Ashton-Alcox, K.A., 2006. How long does oyster shell last on an oyster reef. *Estuar. Coast. Shelf Sci.* 69 (3–4), 531–542.
- Powell, E.N., Klinck, J.M., 2007. Is oyster shell a sustainable estuarine resource? *J. Shellfish Res.* 26 (1), 181–194.
- Puckett, B.J., Eggleston, D.B., 2012. Oyster demographics in a network of no-take reserves: recruitment, growth, survival, and density dependence. *Mar. Coast. Fish.* 4 (1), 605–627.
- Railsback, S.F., 2001. Concepts from complex adaptive systems as a framework for individual-based modelling. *Ecol. Modell.* 139 (1), 47–62.
- Railsback, S.F., Grimm, V., 2019. *Agent-based and Individual-Based modeling: a Practical Introduction*. Princeton University Press.
- Reynolds, C.W., 1987. *Flocks, Herds and schools: A distributed Behavioral Model*, 21. ACM, pp. 25–34.
- Schulte, D.M., Burke, R.P., Lipcius, R.N., 2009. Unprecedented restoration of a native oyster metapopulation. *Science* 325 (5944), 1124–1128.
- Scyphers, S.B., Powers, S.P., Heck Jr., K.L., Byron, D., 2011. Oyster reefs as natural breakwaters mitigate shoreline loss and facilitate fisheries. *PLoS ONE* 6 (8), e22396.
- Sleeman, J.C., Boggs, G.S., Radford, B.C., Kendrick, G.A., 2005. Using agent-based models to aid reef restoration: enhancing coral cover and topographic complexity through the spatial arrangement of coral transplants. *Restor. Ecol.* 13 (4), 685–694.
- Soniat, T.M., Klinck, J.M., Powell, E.N., Cooper, N., Abdelguerfi, M., Hofmann, E.E., Dahal, J., Tu, S., Finigan, J., Eberline, B.S., Peyre, J.F.L., 2012. A shell-neutral modeling approach yields sustainable oyster harvest estimates: a retrospective analysis of the Louisiana state primary seed grounds. *J. Shellfish Res.* 31 (4), 1103–1112.
- Speights, C.J., McCoy, M.W., 2017. Range expansion of a fouling species indirectly impacts local species interactions. *PeerJ* 5, e3911.
- Stephenson, S.P., Sheridan, N.E., Geiger, S.P., Arnold, W.S., 2013. Abundance and distribution of large marine gastropods in nearshore seagrass beds along the Gulf Coast of Florida. *J. Shellfish Res.* 32 (2), 305–313.
- Stempien, J.A., 2007. Detecting avian predation on bivalve assemblages using indirect methods. *J. Shellfish Res.* 26 (1), 271–280.
- Toth, L.T., Stathakopoulos, A., Kuffner, I.B., Ruzicka, R.R., Collella, M.A., Shinn, E.A., 2019. The unprecedented loss of Florida's reef-building corals and the emergence of a novel coral-reef assemblage. *Ecology* e02781.
- Wang, H., Huang, W., Harwell, M.A., Edmiston, L., Johnson, E., Hsieh, P., Milla, K., Christensen, J., Stewart, J., Liu, X., 2008. Modeling oyster growth rate by coupling oyster population and hydrodynamic models for Apalachicola Bay, Florida, USA. *Ecol. Modell.* 211 (1–2), 77–89.
- Watts, D.L., Cohen, M.J., Heffernan, J.B., Osborne, T.Z., 2010. Hydrologic modification and the loss of self-organized patterning in the ridge–slough mosaic of the Everglades. *Ecosystems* 13 (6), 813–827.
- Wilberg, M.J., Wiedenmann, J.R., Robinson, J.M., 2013. Sustainable exploitation and management of autogenic ecosystem engineers: application to oysters in Chesapeake Bay. *Ecol. Appl.* 23 (4), 766–776.
- Yñiguez, A.T., McManus, J.W., DeAngelis, D.L., 2008. Allowing macroalgae growth forms to emerge: use of an agent-based model to understand the growth and spread of macroalgae in Florida coral reefs, with emphasis on *Halimeda* tuna. *Ecol. Modell.* 216 (1), 60–74.
- Young, O.R., 2017. *Governing Complex systems: Social Capital for the Anthropocene*. MIT Press.